Materials Development and Prospective for Protonic Ceramic Fuel Cells

Idris Temitope Bello[a], Shuo Zhai[a], Qijiao He[a], Chun Cheng[a], Yawen Dai[a], Bin Chen[b], Yuan Zhang[b,*], Meng Ni[a,*]

[a] Department of Building and Real Estate, Research Institute for Sustainable Urban Development (RISUD), The Hong Kong Polytechnic University, Hung Hom, Kowloon, Hong Kong, China

[b] Institute of Deep Earth Sciences and Green Energy, College of Civil and Transportation Engineering, Shenzhen University, Shenzhen 518060, China

* Corresponding author: yuanzhang1216@szu.edu.cn (Y. Zhang);

meng.ni@polyu.edu.hk (M. Ni)

Abstract

Protonic ceramic fuel cells (PCFCs) are considered a potential and more efficient upgrade to conventional solid oxide fuel cells (SOFCs). This is predominantly due to their capacity to operate efficiently at low and intermediate temperatures and their quality of non-fuel dilution at the anode during operation. This review presents a detailed exposition of the material development strategies for the major components of PCFCs (i.e., electrolyte, cathode, and anode) and how they differ from the traditional SOFCs. Credible science backed recommendations for the synthesis and fabrication of PCFCs materials are discussed. In the end, the opportunities, challenges, and future directions for P-SOFCs are buttressed.

Keywords: Protonic ceramic fuel cells; cathode; anode; electrolyte; Solid oxide fuel cells

2.1 Introduction

1.1 General overview of O-SOFC and H-SOFC

The past decades have witnessed a progressive surge in global energy demand. The increasing world population and fast-paced urbanization have contributed a great deal to this high global energy demand. Consequently, the emissions associated with the increasing energy consumption have triggered a continuous and unfavorable change to the global climate. Hence, it is of paramount importance to seek an environmentally friendly, clean, and sustainable energy alternative. Renewable energy sources are considered a potential solution to the menacing consequences of global warming on our planet. Some of the widely explored renewable energy sources reported in the literature are solar [1,2], hydroelectric [3,4], wind [5,6], geothermal [7,8], and tidal energy [9,10]. Nevertheless, due to many constraints ranging from the intermittent nature of these common highlighted renewable energy sources to their peculiarities to different geographical locations, as described in [11], make the quest for the development of reliable and large-scale energy conversion and storage technologies a worthy objective. Fuel cells are highly promising energy conversion technologies that convert chemical energy directly to electrical energy with low emission and high efficiency. They are electrochemical systems just like batteries but continue to generate electrical energy supply so long as there is no disruption in fuel and air supply. Fuel cells are of different varieties, and they can be distinguished based on the type of electrolyte used. **Table 1** illustrates the different types of fuel cells developed, their operation temperatures, power outputs, and electrolyte type. Among the different fuel cell types developed, solid oxide fuel cell (SOFC) is the most promising for stationary applications with great potential to replace conventional thermal power plants.

SOFCs are ceramic-based energy conversion systems peculiarly characterized by the direct conversion of chemical energy to electrical energy with low emissions and high efficiency [23]. Some of the advantages of SOFCs over other fuel cell types are fuel flexibility, lower overpotential losses, higher efficiency, and relatively low cost. SOFCs are high temperatures (usually, 800 – 1000 ℃) operating electrochemical conversion systems that could be used for stationary power generation (i.e., either centralized or distributed power generation source) in homes and other areas. The high temperature is needed to enable fast oxygen ion conduction through the dense electrolyte and fast reaction kinetics at the electrodes, especially the oxygen reduction reaction (ORR) at the cathode. However, such a high working temperature also shows several drawbacks [24]. The thermal cycling between room temperature and working temperature may cause substantial thermal stress at the interfaces between different layers due to thermal expansion coefficient (TEC) mismatch, which can severely decrease the performance and durability of SOFC [25]. From a thermodynamics point of view, the maximum theoretical efficiency of fuel cells also decreases with increasing temperature, thus, a too high working temperature is not favorable for the energy efficiency of fuel cells. In addition, high working temperature requires complex and costly thermal management systems and balance of plant (BOP), which raises the overall system cost and hinders the practical applications of SOFC [26]. Hence, it is critical to developing SOFCs that can operate at low to intermediate temperatures (usually in the range of 300 - 750 ℃) [27]. Previous studies have explored and expounded on SOFC components to achieve a cell that can operate at an intermediate and even low temperature [21,28–35]. Some of the strategies prescribed and investigated are the improvement of the electrolyte by using a super-thin (i.e with low ohmic resistance) and the development of high-performance oxygen ion-conducting electrolytes, particularly the doped ceria electrolytes, Gadolinium doped Ceria (GDC), and Samarium doped

Ceria (SDC)[29,36–40]. Another highly efficient strategy is to introduce mixed conductivity into the electrodes such that they can effectively and simultaneously conduct electrons and ions [41–44]. The advantage of this is that the ORR which often takes place at the triple phase boundary (TPB) can be extended to the entire surface of the catalyst particles. These strategies have been quite helpful as evident from myriads of earlier studies reported [45–51].

The cathode is one of the key components to improve to achieve efficient medium and low-temperature operating SOFCs. This is because, it is the site where electrocatalytic ORR takes place, and it influences the stability and durability of the cell. Extensive research has been done to improve the performance, stability, and durability of cathode materials, particularly in oxygen ion-conducting O-SOFCs. Zhou et al. [52] reviewed the progress in improving the popular $Ba_{0.5}Sr_{0.5}Co_{0.8}Fe_{0.2}O_{3-\delta}$ (BSCF) perovskite oxide cathode material that was first reported by Shao and Haile in 2004. BSCF was one of the first reported perovskite oxide materials with an excellent performance at intermediate operating temperatures [53]. Pelosato et al.[54] reviewed over 250 articles highlighting the relevance of cobalt-based double perovskites for intermediate operating solid oxide fuel cells and particularly singling out Pr-, Nd-, Sm-, and Gd-based cobalt-containing layered perovskite oxides as promising candidates for intermediate-temperature SOFCs. Ding et al. [26] also reviewed the use of Ruddlesden-Popper perovskites in intermediate-temperature SOFCs due to their excellent catalytic activity towards ORR and high stability at low and medium operation temperatures.

SOFCs can be classified into oxygen ion-conducting SOFCs (O-SOFCs) and proton-conducting SOFCs (P-SOFCs) depending on the nature of charge carrier(s) in the ceramic electrolyte. Most of the mainstream research in SOFCs is focused on the O-SOFCs in which oxygen ion is the charge carrier in the electrolyte[55–66]. Numerous research works have been done in improving the

performance, stability, and durability of O-SOFCs with remarkable progress being made, particularly in the improvement of the electrode activities of cathode materials for O-SOFC [67–73]. Notable research studies have also been conducted to develop and improve upon the commonly used benchmark for electrode material development (i.e., BSCF) in O-SOFCs [32]. Whilst exerting efforts to achieve a SOFC with high performance, stability, and durability that can operate at intermediate and low temperatures, it is prudent to consider an even more promising alternative. In 1981, Iwahara et al. [74] pioneered the investigation and demonstration of the concept of proton conductivity in perovskite oxide-based materials using $SrCeO_3$ material as electrolyte. This research opened the floodgate of an investigation into the propensity of the viability of proton-conducting electrolyte materials. It was discovered that proton-conducting SOFCs also known as protonic ceramic fuel cells (PCFCs) are more promising in achieving high performance at an intermediate to low temperature [75,76]. Compared to O-SOFCs, there are less reported articles on PCFCs development because it is relatively at the early stage. Over the past years, PCFCs have gradually garnered attention partly because of the certain unique merits they possess such as lower activation energy for proton conduction and potentially lower operation temperature capability. The comparison between O-SOFCs and PCFCs is discussed in detail in **Section 1.2**.

1.2 Comparison between O-SOFC and PCFC

Figure 1 illustrates the schematic of O-SOFC and PCFC. The most distinctive feature which differentiates P-SOFC from O-SOFC is the mode of operation of the electrolyte. The electrolyte of PCFC conducts protons while that of O-SOFC conducts oxygen ions during operation.

O-SOFCs is characterized by the migration of oxygen ions from the cathode side to the anode side through the electrolyte membrane when the air supplied to the cathode is reduced after reacting with the electrons received from the anode via the externally connected circuit.

In contrast to the traditional oxygen ion-conducting SOFC where oxygen ions migrate from the cathode to the anode, the protonic ceramic fuel cells (PCFC) are SOFCs in which the migration species are predominantly protons, which migrate from the anode to the cathode at relatively lower activation energy with the formation of water at the cathode side as illustrated in **Figure 1**. The lower activation energy for the migration of protons through the electrolyte and the formation of water at the cathode is advantageous [77,78]. They give PCFCs an edge over the oxygen ion-conducting SOFC because there will be no problem of fuel dilution at the anode since the water formation will only occur at the cathode. Thus, the unreacted hydrogen fuel can be directly recycled for reuse. In addition, the maximum theoretical efficiency of PCFCs is higher than that of O-SOFC since this theoretical efficiency increases with decreasing temperature. PCFCs are also compatible with multiple fuel types and when hydrocarbon fuel such as methane is used, there can be simultaneous production of electricity and useful byproduct such as ethylene (which helps in the regulation of physiological processes particularly in plant growth) [28,79]. Another interesting benefit of the formation of water at the cathode side is that there will be an easier CO_2 capture and sequestration since the water formed will be separated from CO_2.

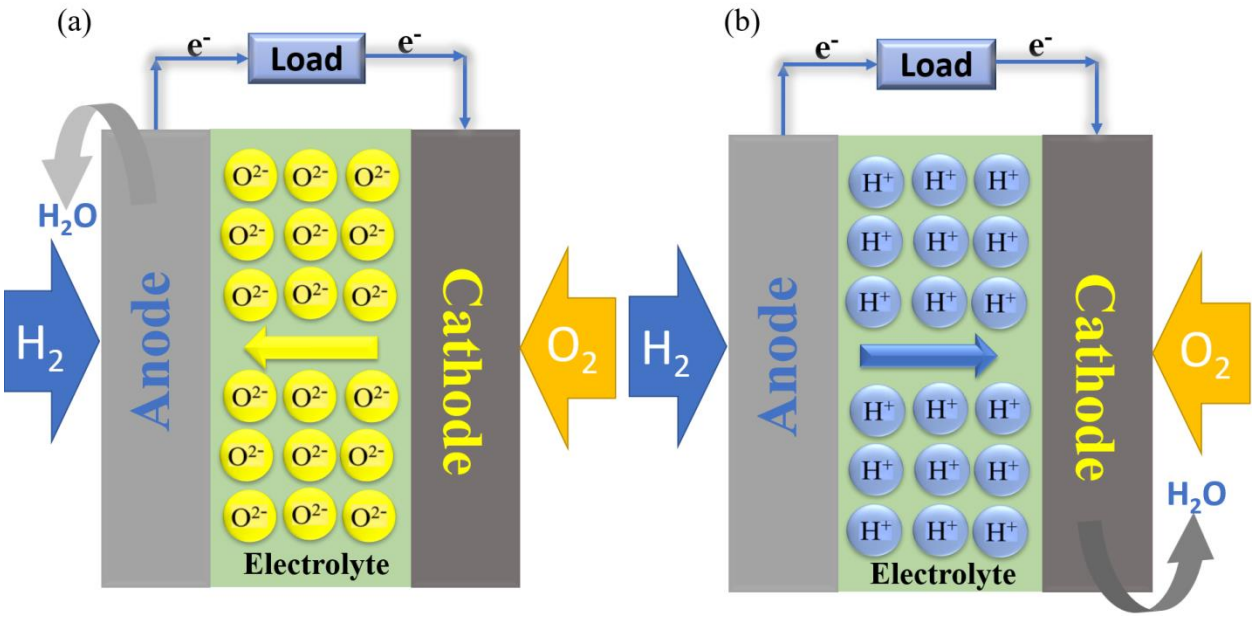

Figure 1: Illustration showing the working principle of solid oxide fuel cells with hydrogen and air being fed to the cell via the anode and cathode, respectively. (a) oxygen ion-conducting SOFC (O-SOFC) and (b) protonic ceramic fuel cell (PCFCs)

Furthermore, several studies have suggested that P-SOFCs have the potential of resisting the poisoning effect of H_2S [80]. However, despite the numerous potentials of PCFC in achieving a state-of-the-art energy conversion technology, there are still certain challenges, particularly with the anodic and cathodic reaction processes, that need to be thoroughly investigated. For instance, there are still issues related to the sintering, conductivity, stability, and durability of PCFC electrolyte materials which are detrimental to the development and commercialization of ceramic fuel cells.

2.2 Extraction of relevant articles related to PCFCs from Scopus database

After the perusal of notable review articles as well as other classical research works in PCFCs such as those of Kreuer [81], Duan et al. [82], Fabbri [83], among others [84], the search string for the

extraction of all related articles to PCFC development was formulated as follows: *(TITLE-ABS-KEY("protonic SOFC*" OR "proton-conducting solid oxide fuel cell*" OR "proton ceramic fuel cell*" OR "proton-conducting ceramic fuel cell*" OR "ceramic fuel cell*" OR "protonic ceramic fuel cell*" OR "solid oxide fuel cell*") AND TITLE-ABS-KEY("proton-conducting*" OR "proton conductive*" OR PCFC OR H-SOFC OR P-SOFC)) AND (LIMIT-TO (DOCTYPE," ar") OR LIMIT-TO (DOCTYPE, "re")) AND (LIMIT-TO (LANGUAGE, "English")).* After the use of this search string in the retrieval of all articles relevant to the subject of interest from Scopus database, manual exercise was carried out to pick the top articles using criteria such as number of citations, relevance of the article abstracts, among others. The articles retrieved were also fine-tuned as illustrated in the search string to be restricted to journal articles and reviews. Based on the outcome of the results from this search the publication trend for PCFC related research is summarily illustrated in **Figure 2.**

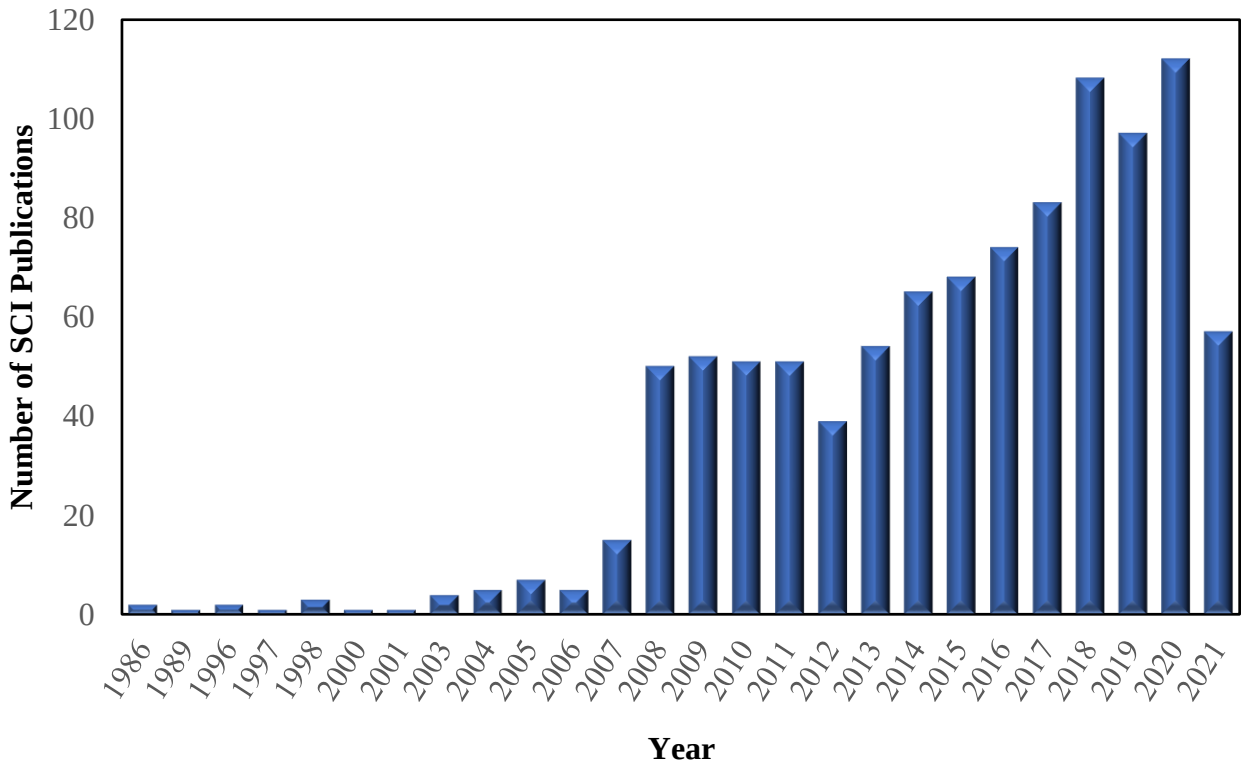

Figure 2: Annual publication trend of PCFC related research from inception till date (2021).

Based on the annual research output in this area, as shown in **Figure 2,** it is evident that there has been a continuous and significant increase in efforts exerted towards the development of protonic ceramic fuel cells which subsequently signals the relevance of this research area.

2.1 Proton conduction mechanisms in PCFC materials

2.2.1 Protonic defects

Proton uptake within the structure of ceramic oxide materials is predominantly due to their oxygen deficient nature induced by either extrinsic or intrinsic defects. The latter are defects attributed to alterations in the material structure (such as the absence of an atom) while the former are defects due to impurities or substitution of the B-site species with acceptor dopants as illustrated in equation (1)[81].

$$Acc_2O_3 + 2B_B^{\times} + 0.5O_2 \rightarrow 2Acc_B' + V\ddot{o} + 2BO_2 \quad (1)$$

where Acc stands for the acceptor dopants which is a trivalent cation and B symbolizes the host specie at the B-site.

The above mechanism is the predominantly observed mechanism for proton defect formation in proton conducting solid oxide electrolysis and fuel cells. However, proton defect can also be formed through another means which involves a non-oxygen defect participating proton incorporation in the presence of hydrogen enriched atmosphere as shown in equation 2.

$$H_2 + 2O_O^{\times} \rightarrow 2OH\dot{o} + 2e' \quad (2)$$

Nevertheless, this latter category of materials is not suitable and used as electrolyte materials because of the formation of electronic defects as compensational charges which eventually triggers electronic conductivity [85].

Hence, in a sodden atmosphere, protonic defects are formed through the dissociation of water into two hydroxyl ions in the presence of oxygen lattice and oxide ion vacancies as illustrated in equation 3. The formation of these hydroxyl ions is due to the covalent bond formation between the lattice oxygen from the structure and a proton, and also as a result of the filling of the oxygen ion vacancy by the other hydroxide ion to form a protonic defect [81].

$$H_2O + O_O^{\times} + V\ddot{o} \leftrightharpoons 2OH\dot{o} \quad (3)$$

where $O_O^{\times}$ symbolizes the lattice oxygen, $V\ddot{o}$ symbolizes the oxygen vacancy and $OH\dot{o}$ represents the proton defect.

Based on Equation 3 which is known as hydration equation, proton uptake involves acid-base reaction involving the dissociative incorporation of water into oxide ion vacancies and it implies that an increase in the partial pressure of water will consequently result in the increase of proton uptake and a decrease in oxygen vacancy concentration. The hydration process can be represented by the law of mass action as shown in equation 4.

$$K_{hydration} = \frac{[\mathrm{OH\dot{o}}]^2}{p_{H_2O}[V\ddot{o}][O_O^{\times}]} \quad (4)$$

2.3 Proton transport mechanism

For decades, the concept of proton transport mechanism in ceramic oxide materials has been long debated and researched. Of all the various mechanisms proposed, the Grotthuss mechanism appears to be the most adopted mechanism. According to this mechanism, the migration of proton is by hopping which is caused by a thermally activated process in the form of rapid rotation and reorientation of proton, and the diffusion of the proton from one neighboring oxygen ion site to the other as illustrated in **Figure 3**. This conception is authenticated by measurements of perovskite oxide H/D isotope-effect as shown in

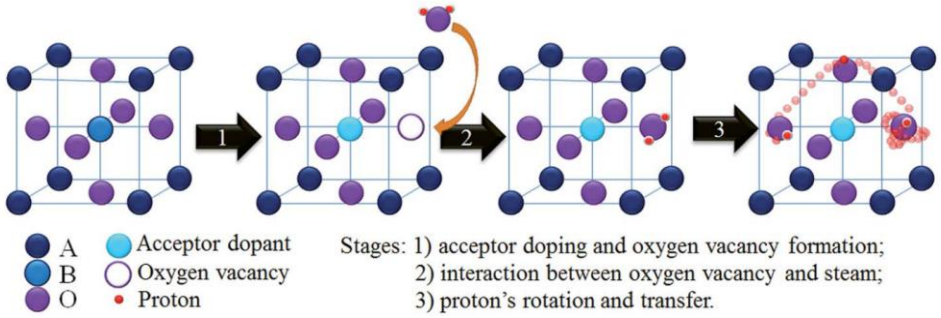

Figure 3: Proton transport mechanism in a typical ABO_3 perovskite oxide material [86]. Copyright 2016, Royal Society of Chemistry.

2.4 Overview of P-SOFC component materials

Just like solid oxide fuel cells, the major components of a protonic ceramic fuel cell are the dense electrolyte, the cathode, and the anode. However, the electrolytes of P-SOFCs conduct protons instead of just oxygen ions as in the case of the traditional O-SOFCs. The electrolyte material must allow easy and swift migration of protons from the anode to the cathode with a very minimal ohmic resistance. For this to occur, the electrolyte material must be dense to ensure maximum conductivity of protons through the electrolyte and minimize reactant crossovers [87]. It is also essential that the electrolyte material possess good chemical and thermo-mechanical compatibility with the other cell components and the atmospheric environment to ensure reasonable stability and durability. **Section 3.0** presents more details about the electrolytes used in P-SOFCs.

On the other hand, the cathode electrode should have excellent diffusion paths and ionic conductivity (i.e., especially for protons) to extend the cathode reaction zone throughout the electrode surfaces. The cathode should also possess good electronic and ionic conductivity to reduce polarization resistance. Likewise, it should possess excellent catalytic activity towards ORR since cathode reactions in proton-conducting solid oxide fuel cells start with oxygen

adsorptive dissociation on the catalyst's surface. The other qualities a good cathode material for P-SOFC should possess are good compatibility with the electrolyte, excellent chemical, and physical stability, and sufficient porosity to provide sufficient transport paths for oxygen and stream molecules. Comprehensive detail of the cathode requirements and other insightful information can be found in **Section 3.2**.

The anode material should possess sufficient porosity (about 20 – 40%) and have a satisfactory conductivity [88]. It is also desirable that the anode material maintains excellent compatibility with multiple fuels such as hydrogen, natural gas, methanol, ethanol, and other hydrocarbons [28,89,90]. It should possess a good surface area with reasonable electrical conductivity and chemical compatibility with adjoining components under reducing conditions at the operating temperature. The anode material should also have a compatible TEC with other cell components as well as sufficient mechanical strength to support the cell, in the case of anode-supported cells [91]. See **Section 3.3** for more details about the anode materials for P-SOFCs.

The early P-SOFCs were high-temperature proton-conducting SOFCs. They were often referred to as high-temperature proton conductors (HTPCs) to differentiate them from polymer electrolyte membrane fuel cells (PEMFCs) that operate at low temperatures (< 100 degrees Celsius). However, attention is currently shifted to intermediate and low temperature operating P-SOFCs. This is because it is cheaper and can potentially increase the durability of SOFC cell components thereby hastening the commercialization process. Attempts have been made to develop intermediate to low temperature operating oxygen ion-conducting solid oxide fuel cells, but this has been challenging. Another viable alternative that has drawn much attention lately is the proton-conducting solid oxide fuel cells. It is quite advantageous to O-SOFC on many fronts. It has lower activation energy and has been reported to be coking and sulfur resistant in reputable studies.

Despite the benefits of P-SOFCs, research is still ongoing to improve their performance, stability, and durability.

2.5 Naming conventions for PCFC materials

Duan et al. [90] proposed a naming convention for the various material's stoichiometric compositions to facilitate uniformity and understanding among various researchers focused on P-SOFC research. If the compound is in the form of $BaCe_{1-x}Y_xO_{3-\delta}$ and $BaZr_{1-x}Y_xO_{3-\delta}$, it should be represented with BCYX and BZYX, respectively and the value of X should be $x \times 100$. For instance, the abbreviation for $BaCe_{0.8}Y_{0.2}O_{3-\delta}$ will be BCY20 and that of $BaZr_{0.8}Y_{0.2}O_{3-\delta}$ will be BZY20. For other categories of compounds in form of $BaZr_{1-x-y}Ce_yY_xO_{3-\delta}$, the format of the abbreviation will indicate the B-site major constituent. If $y < 1 - x - y$, then Zr will be the major B-site constituent and the short form will be BZCYTY, where $T = (1 - x - y) \times 100$. However, if $y > 1 - x - y$, then Ce will be the major B-site constituent, and the abbreviation will be in the form BCZYYT, where $Y = y \times 100$ and $T = (1 - x - y) \times 100$. For instance, the abbreviations for $BaCe_{0.6}Zr_{0.2}Y_{0.2}O_{3-\delta}$ and $BaZr_{0.6}Ce_{0.2}Y_{0.2}O_{3-\delta}$ will be BCZY62 and BZCY62, respectively. Finally, if the compound happens to be in the form of $BaZr_{1-x-y-z}Ce_yY_xYb_zO_{3-\delta}$, it will follow the same rule as in $BaZr_{1-x-y}Ce_yY_xO_{3-\delta}$ compounds earlier described with only an exception that all the percentage constituent of all the B-site compositions will reflect. For instance, the abbreviation of the compounds $BaZr_{0.4}Ce_{0.4}Y_{0.1}Yb_{0.1}O_{3-\delta}$ and $BaZr_{0.7}Ce_{0.1}Y_{0.1}Yb_{0.1}O_{3-\delta}$ will be BZCYY4411 and BZCYYb7111, respectively.

3.0 Materials development for various components of PCFCs

3.1 Electrolyte materials

Decades of research have revealed that the best protonic ceramic oxide materials are ABO_3 structured perovskite oxides in which the A-sites are predominantly filled with alkaline earth metals or rare metals with relatively large ionic sizes such as Ca, Sr, Ba and La while the B-sites are dominated by smaller sized tetravalent elements such as Zr and Ce [92,93,93–95]. These materials are relatively stable and exhibit a high level of proton conductivity. Ba for instance, has a large ionic size and for this reason, it is an A-site dominant material whereas Ce and Zr are B-site dominant cations, respectively. When B-sites of these proton conducting materials are doped with extrinsic trivalent elements (i.e., impurities) such as Yb, Y, Gd, In, among others, they will create oxygen vacancies in the material which will in turn enhance the proton conductivity of the material. **Error! Reference source not found.** illustrates the unit cell ABO_3 structure of a typical proton conducting perovskite oxide electrolyte material. Section 2.1 Proton conduction mechanisms in PCFC materialsdiscusses the mechanisms of proton conduction Figure 4: ABO_3 structure of a

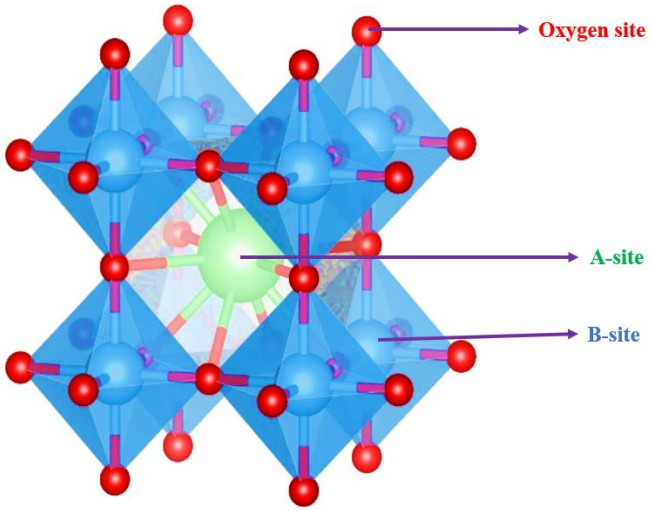

typical protonic ceramic electrolyte material and transport in proton conducting ceramic materials.

A summary of the electrochemical performances of P-SOFC single cells with proton conducting electrolyte materials is presented in **Table 2**.

3.1.1 Proton Conductivity and Stability of ceramic oxide electrolyte materials

3.1.1.1 Barium cerate-based materials

$BaCeO_3$ based oxides are one of the most explored perovskite oxide materials for proton-conducting electrochemical systems [84,96–102]. These materials exhibit mixed conductivity (i.e., ionic, and protonic) and they find application in various systems such as steam electrolyzers for hydrogen production, and electrolytes for proton-conducting solid oxide fuel cells. The proton conductivity in this category of protonic electrolyte materials stems from the interaction between oxygen vacancies and water vapor as described in [103]. Furthermore, an early investigation of proton conductivities of various perovskite oxide-based materials such as indates, hafnates, scandates, yttrates, tantalates, zirconates of alkali-earth elements, and barium cerates, confirms that those based on barium cerates have the highest conductivities [81,104]. The higher proton conductivity in $BaCeO_3$ based oxides (i.e., 10^{-2} S cm^{-1} at 600 ^oC[105]) could be due to their relatively low electronegativities, larger ionic radii due to the Ba cation in their A-sites, or/and their lower grain-boundary resistance on the overall resistance of the perovskite oxide material [96]. Also, studies have confirmed that $Sr/CaCeO_3$ and $Sr/CaZrO_3$ based oxides have poor hydration capability and lower proton conductivity compared to $BaCeO_3$ based oxides as shown in **Figure 4**.

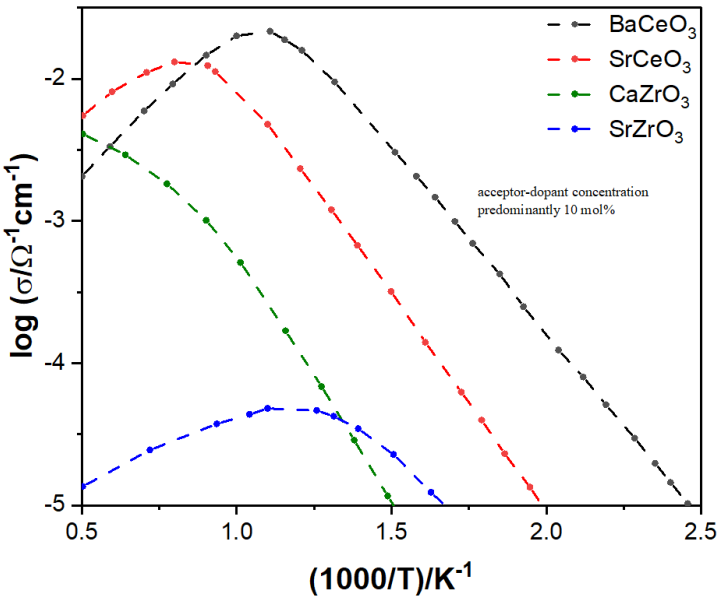

Figure 4: Proton conductivities of $BaCeO_3$ electrolyte material relative to other protonic ceramic materials [81].

However, later studies suggested that the high proton conductivity in $BaCeO_3$ based oxides should not be the major yardstick in concluding the viability of their application in electrochemical systems due to their low stability in water and other acidic compounds [101,103,106]. Also, Bhide et al. [107] confirmed that $BaCeO_3$ based electrolyte materials have poor stability relative to other electrolyte materials as shown in **Figure 5**. $BaCeO_3$ based materials have reaction affinity for atmospheric gases (such as illustrated in equations 5-8) and this causes the cerate phase to be decomposed. Equations 5 – 8 show what happens when $BaCeO_3$ reacts with water or any acidic compound.

$$BaCeO_3 + H_2O \rightarrow Ba(OH)_2 + CeO_2 \quad (5)$$

$$BaCeO_3 + CO_2 \rightarrow BaCO_3 + CeO_2 \quad (6)$$

$$BaCeO_3 + SO_2 \rightarrow BaSO_3 + CeO_2 \quad (7)$$

$$BaCeO_3 + H_2O \rightarrow BaS + H_2O + CeO_2 \quad (8)$$

Due to the challenges encountered with the use of $BaCeO_3$ based oxides as electrolyte materials for proton-conducting solid oxide fuel cells, efforts were channeled toward developing materials with excellent mixed conductivity and satisfactory stability against water and acidic atmospheres[81,86,93,108–114]. Some of those strategies employed were (i) co-doping of $BaCeO_3$ using various suitable elements which could either be metallic or non-metallic, (ii) introduction of phases with high stability properties to the $BaCeO_3$ based material in the form of composite material development. Based on the outcome of various research works, zirconium was found to be the most suitable element to improve the stability of $BaCeO_3$ [98], although at the expense of other electrical properties of the material as will be discussed in the next section.

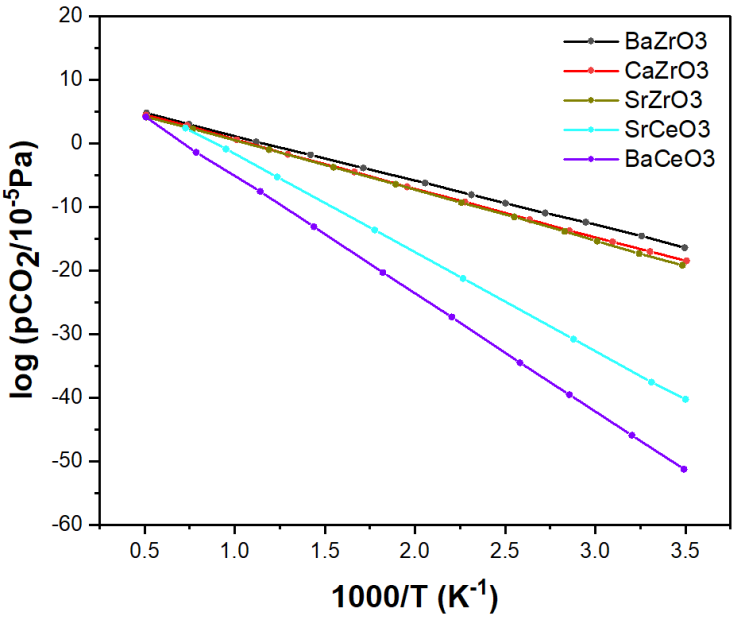

Figure 5: Stability of various proton conducting electrolyte materials based on different pCO_2 and temperatures reproduced from [115]. Copyright Elsevier, 2008.

3.1.1.2 Barium zirconate-based electrolyte materials

It has been established that the cerate-based perovskite oxide materials exhibit the highest protonic conductivity among all other perovskite oxide materials, with $BaCeO_3$ based oxides being the category of cerates with the highest conductivity. Nevertheless, they are very unstable under practical conditions in electrochemical systems. The Zirconium-based oxides on the other hand are reputable for their high stability under various acidic and atmospheric conditions. $BaZrO_3$ based oxides are chemically stable in water and CO_2 environments. Lu et al. [115] established the relationship between increasing partial pressure of CO_2, Zr content, x and equilibrium reaction temperature of $BaCe_{1-x}Zr_xO_3$. They confirmed that the stability of $BaCe_{1-x}Zr_xO_3$ increases with increasing Zr content, x at a given CO_2 partial pressure as illustrated in **Figure 6**.

Furthermore, $BaCeO_3$ and $BaZrO_3$ based oxides have ionic conductivities in the range of 10^{-2} and 10^{-1} S cm^{-1} at low and intermediate temperatures[116,117]. However, certain challenges limit their application as electrolyte materials in proton-conducting solid fuel cells. $BaZrO_3$ based oxides have issues of significant grain boundary resistance and poor sintering.

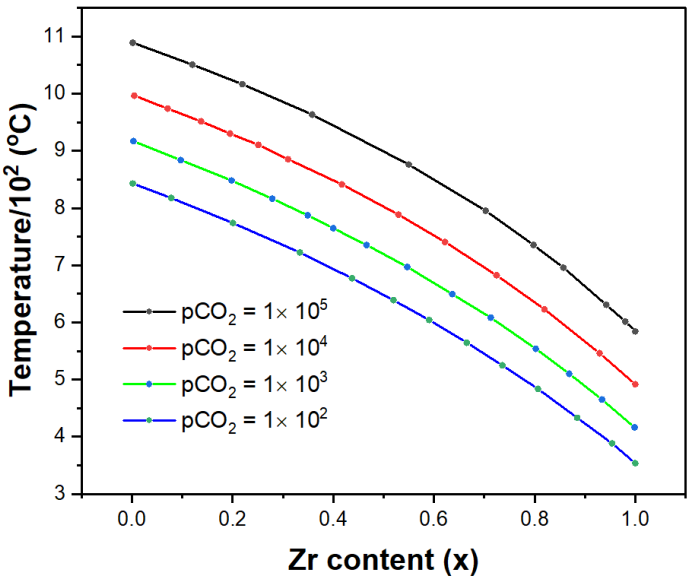

Figure 6: Effect of Zr content and partial pressure of CO_2 on equilibrium reaction temperature of $BaCe_{1-x}Zr_xO_3$, reproduced from [115]. Copyright 2008, Elsevier.

3.1.2 Grain boundary characteristics of PCFC electrolyte materials

One of significant influencing factors affecting the conductivities of proton conducting solid oxide fuel cells is their grain boundary characteristics[118–121]. Grain boundary resistance has been identified to be a problem, particularly to the conductivity of $BaZrO_3$ based oxides. Hence, as a rule of thumb, as the grain size increases, the material conductivity increases and vice versa. $BaZrO_3$ based oxides on the other hand are characterized by small sized grains at the grain boundaries which is responsible for their high grain boundary resistances and low conductivity [122]. Grain boundary architecture is often influenced by segregation forces causing acceptor dopants to accumulate around materials grain boundary core as well as depleting oxygen vacancies and protons. The consequence of this interaction is the formation of space effects that influence the transport of ions as shown in **Figure 7**.

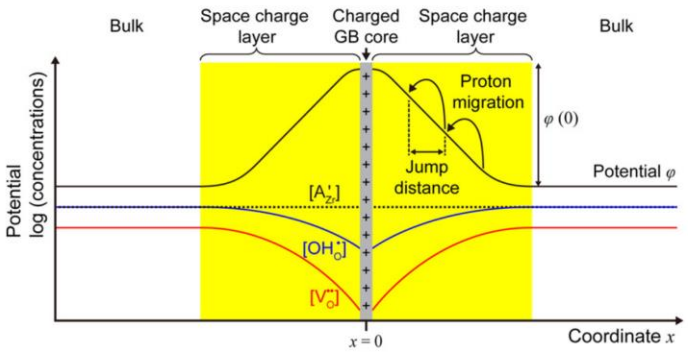

Figure 7: Space charge layer model at the grain boundary core of a typical PCFC electrolyte material. Copyright 2013, Elsevier.

Iguchi et al. [123] investigated the effects of grain boundary diameter and microstructure on the electrical conductivities of $BaZrO_3$ based oxides. They particularly considered Y-doped $BaZrO_3$ prepared by solid state reaction process and Pechini method subjected to different sintering conditions. It was confirmed that the electrical conductivity of the material was significantly affected by the duration of sintering with the sample subjected to 200 h sintering time exhibited the lowest electrical conductivity. However, the sample preparation methods had no effect on the grain boundary characteristics [123]. Y-doped $BaZrO_3$ with 20% doping level have been widely used and considered to be excellent candidates for PCFC electrolytes. However, the percentage level of doping of $BaZrO_3$ with Y (i.e., BZY20) often leads to the formation of secondary phase (i.e., BaY_2NiO_5) thereby compromising the BZY20 as shown in Figure 8. This implies that the subsequent co-sintering of the supposed BZY20 with NiO will no longer be a 2-phase equilibrium comprising just BZY20 and NiO. Hence, it is proposed that this problem can be solved by limiting the doping level of Y in BZY20 to a maximum of 12% or introducing other dopants such as Yb [124]. The phenomenon described involving foreign phase formations significantly affects the transport of ions around the grain boundaries [125].

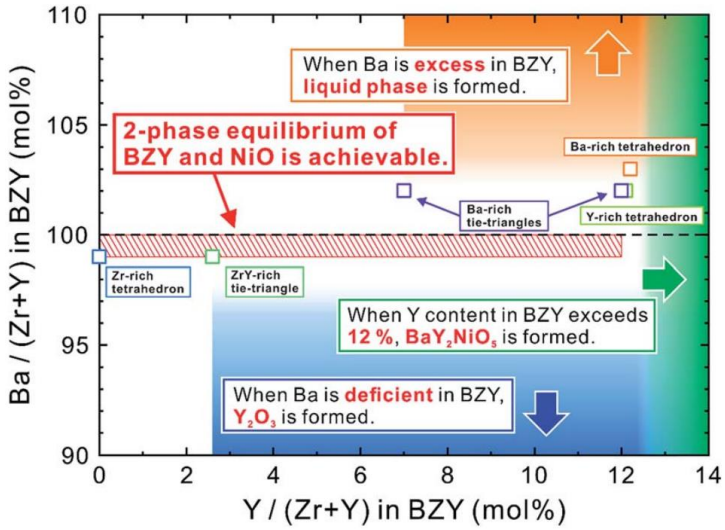

Figure 8: Expected secondary phases to be formed when various BZY compositions are co-sintered with NiO [124]. Copyright 2019, Royal Society of Chemistry.

3.1.3 Sintering of PCFC electrolyte materials

As earlier discussed in the previous section concerning grain boundary resistant problem of $BaZrO_3$ based oxide, various approaches have been employed to address this challenge. The use of several sintering aids such as NiO, ZnO, CuO, etc., have been proposed [126–128]. However, Han et al. [112] and others suggested that the use of sintering aids such as NiO, ZnO, and CuO impedes the proton conductivity in BZY20 and leads to the creation of hole conduction in an oxidizing atmosphere [127,129,130]. The most investigated doped $BaZrO_3$ oxide is yttrium doped barium zirconate, BZY. There have been co-doping strategies of yttrium barium zirconates with other elements such as Nd, In, Sn, Pr, and Yb to improve the sintering and proton-conducting properties of barium zirconates which has led to certain promising outcomes [131,132]. Asides from the introduction of sintering aids to barium zirconates and co-doping strategies, the use of PLD has also been used to improve the sintering of barium zirconates by Pergolesi et al.[133]. However, PLD is an expensive method and not suitable for large-scale applications. Due to the

various challenges enumerated, an alternative approach to getting a superior proton-conducting electrolyte for P-SOFCs will be a natural combination of yttrium doped barium cerate and yttrium doped barium zirconate to get cerium and yttrium doped barium zirconates as will be explored in the subsequent section.

3.1.4 Other Materials and Challenges

The combination of BCY and BZY has been identified to be a promising approach to getting an improved proton-conducting electrolyte for P-SOFCs. Katahira et al. [98] investigated the effects of variations in the constituents of BCZY. They observed that increasing the Zr content increases the stability of the compound against CO_2 but sacrifices conductivity. Likewise, they varied the Ce content and confirmed that its presence increases the conductivity and sinterability of BCZY. Overall, they concluded that BCZY is stable with an acceptable conductivity. For instance, Zuo et al. [134] investigated the conductivity and stability of BCZY712 at a low temperature of 500 ^oC. It was discovered that BCZY712 exhibited excellent ionic conductivity of 0.009 S cm^{-1} which surpassed that of LSGM, GDC, and YSZ. Likewise, in terms of stability, the structure of BCZY712 was confirmed to be the same before and after exposure to CO_2, H_2O, and CO_2 and H_2O. Another innovative product of the combination of BCY and BZY is BCZY442 [135]. This electrolyte material was reported to have a high bulk proton conductivity and an excellent tolerance to CO_2. However, the challenge with is material lies in its high sintering temperature and low grain boundary proton conductivity [136]. Other approaches that have been employed by researchers are the introduction of several dopants to the B-sites of BCY and BZY. An example of a breakthrough with this approach is the development of BCZYYb7111 in 2009 by Yang et al [137]. The introduction of Yb into BCZY improved the conductivity and stability of BCZY against sulfide and other hydrocarbons. Later studies revealed that CO_2 affects the stability of BCZYYb7111. The

exceptional discovery of another stoichiometric manipulation of BCZY by Choi et al. [138] gave rise to BCZYYb4411. This material was reported to have a high tolerance for CO_2, and this was attributed to the higher content of Zr. Also, the material has relatively improved performance with high resistance to coking and sulfur atmospheres.

3.2 Cathode Materials development for PCFCs

The cathode is the most explored research area in ceramic fuel cell development because of the high activation loss for ORR at the cathode during low and intermediate temperature operating conditions. Thus, developing highly active and stable cathode materials could contribute significantly to the performance improvement of PCFCs. Unlike the case of oxygen ion conducting solid oxide fuel cells where the cathode reaction involves oxygen adsorptive dissociation on the catalyst surface followed by the diffusion of oxygen ions to the anode through the electrolyte, in PCFCs, the oxygen adsorptive dissociation first occurs on the catalyst surface, after which the oxygen ions react with the protons that migrated from the anode through the electrolyte to form water. Equations 9 and 10 illustrate the adsorptive dissociation reactions in O-SOFC and PCFCs, respectively. Detailed stepwise elementary reactions at the cathode for P-SOFCs are presented in **Table 3** while the reaction pathway for a single-phase proton, electron, and oxygen ion-conducting cathode material for proton-conducting solid oxide fuel cells is illustrated in **Figure 9**.

$$O_2 + 4e^- \rightarrow 2O^{2-} \quad (9)$$

$$O_2 + 4e^- + 4H^+ \rightarrow 2H_2O \quad (10)$$

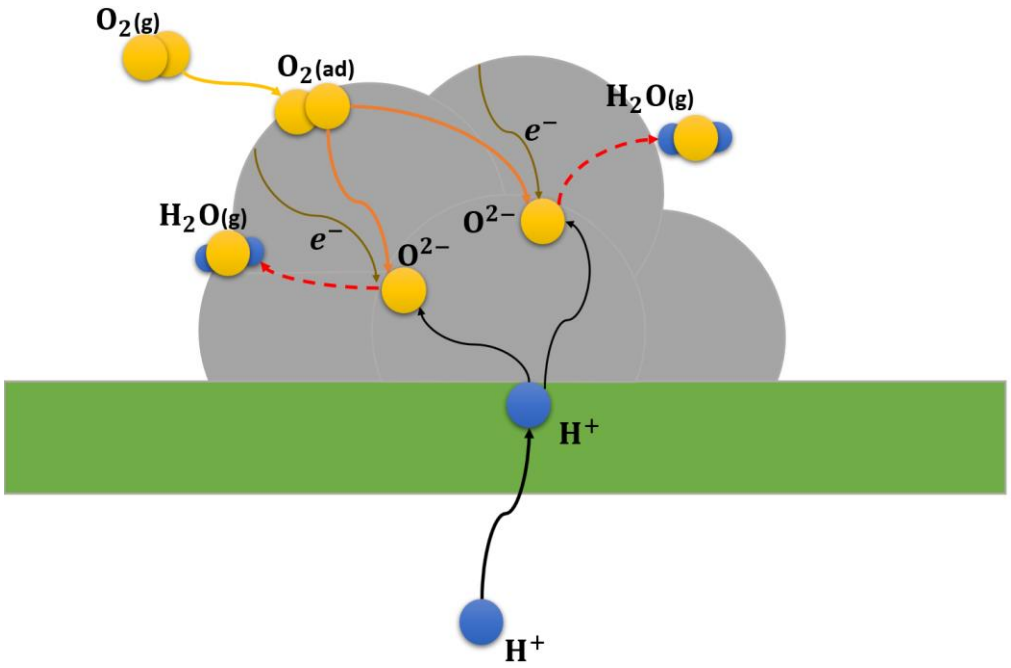

Figure 9: Schematic illustrating reactions in a single-phase triple conducting P-SOFC cathode.

The transfer mode in PCFC cathodes can be divided into four categories; the electron-conducting single-phase cathodes, the proton and oxygen ion-conducting cathodes (i.e., either single-phase or composite material), the oxygen and electron-conducting (MIEC) cathodes (i.e., as a single-phase or composite material) and the proton-electron-oxygen ion-conducting single-phase cathodes (i.e., as shown in **Figure 9**. A schematic illustration of the different transfer modes of cathode materials in P-SOFC is presented in **Figure 10**.

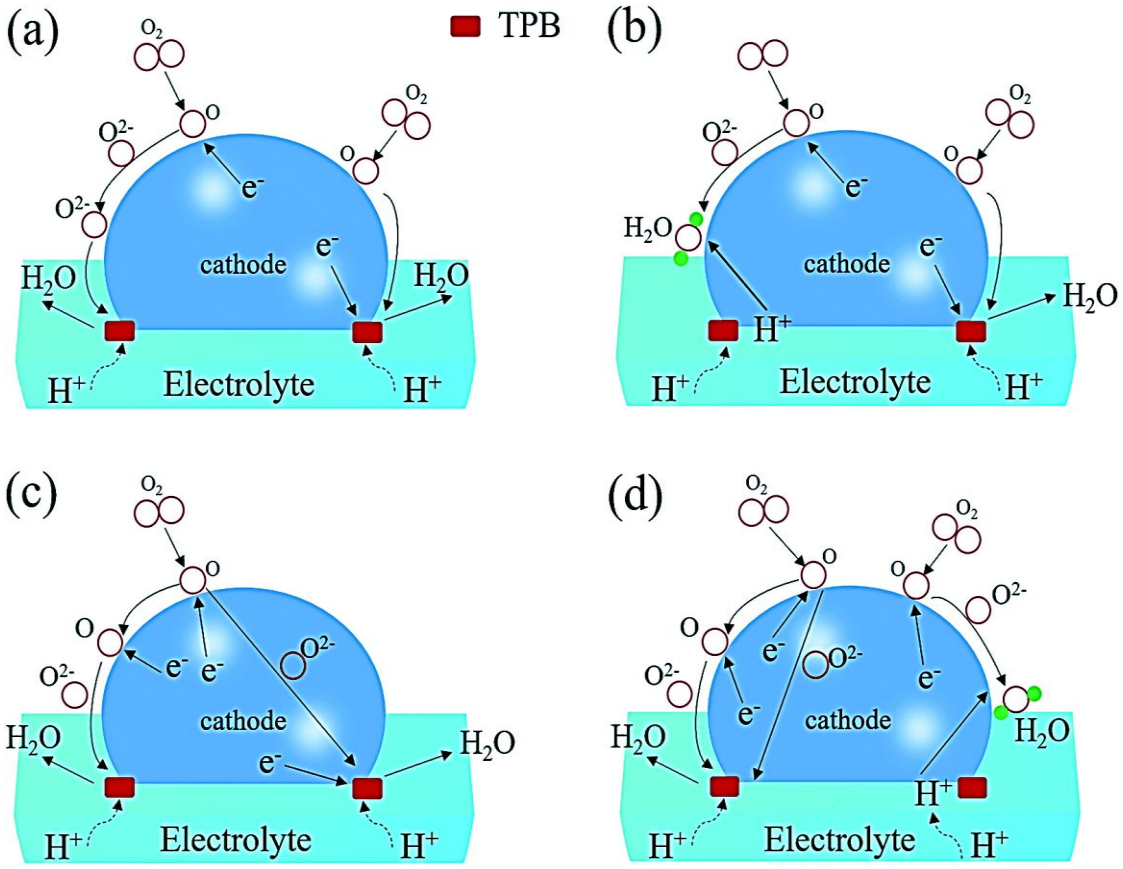

Figure 10: Cathodic reactions in PCFCs [147] for (a) Single-phase electron-conducting cathode materials, (b) proton and oxygen ion-conducting cathode materials, (c) MIEC cathode materials, and (d) proton, electron, and oxygen ion-conducting cathode materials. Copyright 2018, Royal Society of Chemistry.

The foundational concepts for the development of cathode materials for proton-conducting solid oxide fuel cells stem from the knowledge of cathode development for oxygen ion-conducting solid oxide fuel cells. In the conventional SOFCs, what is currently prominent is the development of single-phase mixed ionic and electronic conducting (MIEC) cathodes which are different from the early traditional SOFCs where cathode reactions are limited to the triple-phase boundary (i.e., the interface where oxygen ion, electrolyte, and cathode coincide)[28,148]. The MIEC concept in SOFCs gives the possibility of extending the reaction zone beyond the TPB to the whole surface

of the cathode depending on the efficacy of the cathode constitutive elements [25,149]. Some of the most outstanding results of cathode materials developed for SOFC with MIEC are $Ba_{0.5}Sr_{0.5}Co_{0.8}Fe_{0.2}O_{3-\delta}$ (BSCF)[150] and $La_{0.6}Sr_{0.4}Co_{0.2}Fe_{0.8}O_{3-\delta}$ (LSCF)[151]. Besides these materials developed, other categories of materials developed in later years are double perovskites (i.e., $AÁB_2O_{5+\delta}$ based oxides such as $PrBaCo_2O_{5+\delta}$ [152]), Ruddlesden-Popper (i.e., $A_{n+1}B_nO_{3n+1}$ based oxides such as $La_2NiO_{4+\delta}$ [153]) phases and layered ferrites [154] (e.g., $Sr_2Fe_2O_5$). Other procedures developed to improve oxygen exchange rate by controlling the cathode morphology include in situ exsolution[110], impregnation[155,156], and atomic layer deposition[44].

P-SOFCs and PCFCs share certain common requirements in cathode development, such as consideration of cost of constituent cathode materials, compatibility with other cell components, stability, durability, and performance. Some other requirements such as proton conductivity, among others are peculiar to PCFCs.

3.2.1 Activity

For PCFCs, it is essential that the cathode material possesses effective proton diffusion paths to extend the reaction zone to a higher specific area of active sites which implies that a PCFC cathode material should have a high catalytic activity towards oxygen reduction reaction (ORR) [157]. The cathode catalyst should be capable of effectively dissociating the adsorbed oxygen on its surface for further reactions at the cathode. One of the strategies for increasing the catalytic activity of PCFC cathode material is therefore substituting the A-sites with lower valence ions which have proven to increase electronic conductivity and oxygen adsorptive dissociation. Hence, proton conductivity in PCFCs can be achieved by either introducing proton conductivity into an existing conventional MIEC cathode as in the case of $BaCe_{0.8}Sm_{0.2}O_{2.9}$ being introduced into

$Sm_{0.5}Sr_{0.5}CoO_3$ to achieve a proton-conducting composite cathode with a highly reduced polarization resistance[158]. Another way of achieving a highly active proton-conducting cathode material is by designing single-phase oxides with a triple conducting capability (i.e., proton, oxygen ion, and electron conductivity) as illustrated in **Figure 10 (d)** and **Figure 9**. This oxide should at least have a conductivity of 1 S/cm to ensure excellent performance. In this case, the reaction is extended to the entire surface of the cathode which in turn improves the catalytic activity of the cathode. The stepwise reaction paths for these novel P-SOFC cathodes with triple conductivity are summarily described in **Table 3**.

Kim et al. [159] developed a single-phase cathode material with triple conductivity, $NdBa_{0.5}Sr_{0.5}Co_{1.5}Fe_{0.5}O_{5+\delta}$ (NBSCF). A low polarization resistance of 0.081 Ωcm^2 was achieved at a temperature of 700 ^oC [159]. Also, proton-conducting cathode materials can be derived from proton-conducting electrolytes such as $BaZrO_3$ and $BaCeO_3$ based electrolytes. The electronic conductivity and catalytic properties of the proposed cathode materials can be improved by doping the B sites of proton-conducting electrolytes with highly catalytic elements such as Co and Fe as in the case of $BaZr_{1-x}Co_xO_{3-\delta}$ [160] and $BaZr_{1-x}Fe_xO_{3-\delta}$. In 2015, Duan et al. [82] developed the novel cathode material, $BaCo_{0.4}Fe_{0.4}Zr_{0.1}Y_{0.1}O_{3-\delta}$ (BCFZY0.1). This cathode material was reported to have an excellent ORR at low and intermediate temperatures. When hydrogen fuel was used, the peak power density (PPD) was 455 mW cm^{-2} at a low temperature of 500 ^oC and when methane fuel was used, the PPD was 142 mW cm^{-2} at the same temperature. In 2021, Liang et al. [161] doped the high performance BCFZY cathode material with 5% Ni. This dopant interestingly improved the ASR and PPD of BCFZY material in both P-SOFC and PCFC as illustrated in Figure 11. Another interesting strategy for achieving a high activity in PCFC cathode materials is through the design of self-assembled nanocomposite cathode materials. Self-assembly design of cathode

materials is a novel and emerging approach for preparing composite cathode materials with desirable qualities ranging from high activity to excellent thermo-mechanical compatibility with other cell components. This strategy has earlier been used in the preparation of cathode materials with excellent MIEC in O-SOFCs. For instance, Qi et al. [162] employed the strategy of self-assembly cathode design to prepare cubic-hexagonal perovskite nanocomposites (i.e., $BaCo_{0.6}Zr_{0.4}O_{3-\delta}$ (BZC-BC) nanocomposite comprising cubic $BaZr_{0.82}Co_{0.18}O_{3-\delta}$ (BZC) and 12H hexagonal perovskite material, $BaCo_{0.96}Zr_{0.04}O_{2.6-\delta}$ (12H-BC)) for O-SOFC. The material exhibited an excellent compatibility (i.e., TEC) with GDC electrolyte also a high PPD of 1094 mW cm^{-2} at 650 ^{o}C. Recently, Song et al. [163] employed the self-assembly cathode design approach to prepare a nanocomposite cathode material comprising different phases, proton and electronic conductor phase, $BaCe_xY_yCo_zO_{3-\delta}$ (P-BCCY), the MIEC phase, $BaCo_xCe_yY_zO_{3-\delta}$ (M-BCCY) and another MIEC phase, $BaCoO_{3-\delta}$ (BC). The different inherent phases are entwined to achieve a highly active triple conducting material with the active sites extended throughout the cathode material. At 550 ^{o}C, a high PPD of 508 mW cm^{-2} was achieved which was stable for over 800 h. Despite the significant progress that has been made in the development of P-SOFC cathodes, the electrochemical processes on the cathode need to be further investigated.

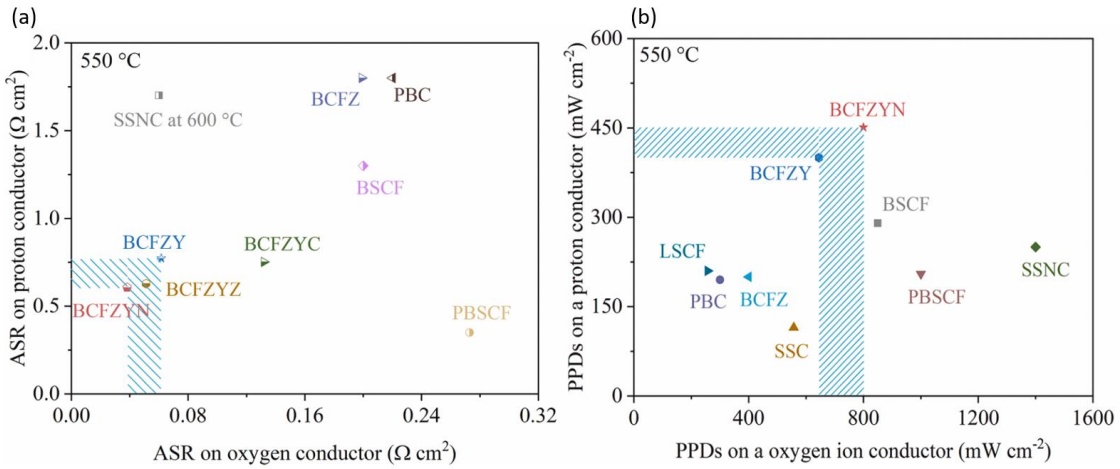

Figure 11: The performance of BCFZYN and other classical electrode materials used in both O-SOFCs and PCFCs, respectively (a) ASR in air with SDC and BZCYYb electrolyte (b) PPD with Ni + SDC │SDC │cathodes and Ni + BZCYYb │BZCYYb │cathodes[161]. Copyright 2021, Elsevier.

3.2.2 Conductivity improvement strategies for PCFC cathode materials

Another essential requirement for P-SOFC cathode material is good electronic conductivity. This is important to achieve a cathode material with low ohmic resistance. The idea of electronic conduction stems from the formation as well as the transportation of electron holes which are achieved through the introduction of transition elements (i.e., Ni, Mn, Fe, Co) in the B-site. The electron holes can be further increased by substituting ions with lower valences as in the case of Ba^{2+}, $Ca^{2+,}$ and Sr^{2+} in the A-site[164]. Furthermore, Zohourian et al. [165] and Papac et al. [166] buttressed on mixed and triple conductivity of cathode materials for P-SOFCs by emphasizing on proton uptake mechanisms in perovskite oxide materials which has been elaborately discussed in section 3.1.1. To develop and design a high-performance cathode material with superb proton, electron, and oxygen ion conductivity for PCFCs, certain strategies have been suggested in the literature[90,109,167]. The materials that are reported to be most suitable for achieving excellent triple conducting single-phase cathodes are either $ABO_{3-\delta}$ perovskites, $A\acute{A}B_2O_{5+\delta}$ double

perovskites, and $A_{n+1}B_nO_{3n+1}$ Ruddlesden-Popper with their A and B sites doped with elements such as Ba, Sr, Zr, Cu, Mn, Co, and Ni[26,77,168–173]. It is best to consider materials with cubic structures and large lattice volumes because they enhance hydration and proton conduction. It is also essential when selecting dopants to consider transition metals with multiple oxidation states because that will significantly enhance redox capability and good electronic conductivity. The B-site cation should possess higher electronegativity than the A-site cation to promote proton uptake and lattice hydration as in the case of specific elements such as Zn, Y and Zr [165]. Also, the A-site cation should have a larger ionic radius to increase the lattice volume, oxygen vacancy concentration, and mobility. Furthermore, the A-site dopants should be carefully selected because this greatly influences the stability and performance of the material. **Table 4** shows a list of recent articles with new findings related to cathode material development for P-SOFCs.

3.2.3 Compatibility with other cell components

A good PCFC cathode material should possess excellent compatibility with the proton-conducting electrolytes, including chemical compatibility and compatibility in thermal expansion coefficient (TEC). The TEC of the cathode material must match reasonably with that of the electrolyte to prevent large thermal stress during thermal cycling, which causes the delamination of the cathode from the electrolyte. The TEC of the cathode materials should be reasonably close to those of the electrolytes, usually in the range of 10^{-6} K^{-1}. Past research studies have revealed that Co-based materials usually have good electrocatalytic activity but also significantly higher TECs than those of Mn-based materials. Hence, reducing the percentage of cobalt in cathode materials by partially replacing it with transition metals can cause a reduction in the material's TEC. Recently, a novel TEC offset approach was proposed by compositing the Co-containing cathode materials with negative thermal expansion (NTE) materials to reduce the overall TEC [174]. As a result, high-

performance and durable cathode materials were developed. Although the cathode was for O-SOFC, the same strategy can be applied to H-SOFC as well.

3.2.4 Chemical and physical stability

Stability is one of the essential yardsticks to assess the quality of a cathode material used in proton-conducting solid oxide fuel cells. Any material selected to be used as a cathode for P-SOFC must possess reasonable chemical stability in CO_2, humid air, etc. Ba and Sr are common A-site elements in cubic ABO_3 and double perovskites used as cathodes in P-SOFCs because of their large ionic size and effect on promoting better oxygen pathways. However, these alkaline earth metals are susceptible to reacting with CO_2 in acidic gases-containing environments thereby causing degradation in the performance of the fuel cell. Despite stability being a crucial quality in PCFC cathodes, its development has drawn less attention compared to the effort exerted on improving the performance of PCFC cathodes. Several articles have confirmed that using monovalent ions such as Zr^{4+}, $Hf^{4+,}$ and Yb^{3+} to dope cathode materials can significantly enhance the stability and activity of the cathode material. Tsvetkov et al. [185] hypothesized and investigated if the use of less reducible cations such as Hf^{4+}, Zr^{4+}, Ti^{4+}, $Nb^{5+,}$ and Al^{3+} can influence the stability of a model perovskite material, $La_{0.8}Sr_{0.2}CoO_3$ (LSC). The outcome of the study revealed that these less reducible cations not only improved the stability but also the oxygen exchange kinetics. Also, another potential aspect that could adversely affect the stability of cathode electrode material is the TEC mismatch between the cathode material and other cell components such as the anode and electrolyte. This is a particularly challenging aspect in cathode material development in both conventional SOFCs and PCFCs. For instance, **Figure 123** illustrates a schematic of various perovskites materials used as either cathode, electrolyte, or anode material for the conventional SOFCs. It is clear from the schematic that different material categories have

disparate TECs. Hence, stability does not necessarily increase the ORR but rather, it ensures the durability of the cathode material. For instance, cobalt-based cathodes are found to possess better ORR and hence better performance, but they exhibit relatively poorer stability compared with cobalt-free cathode materials.

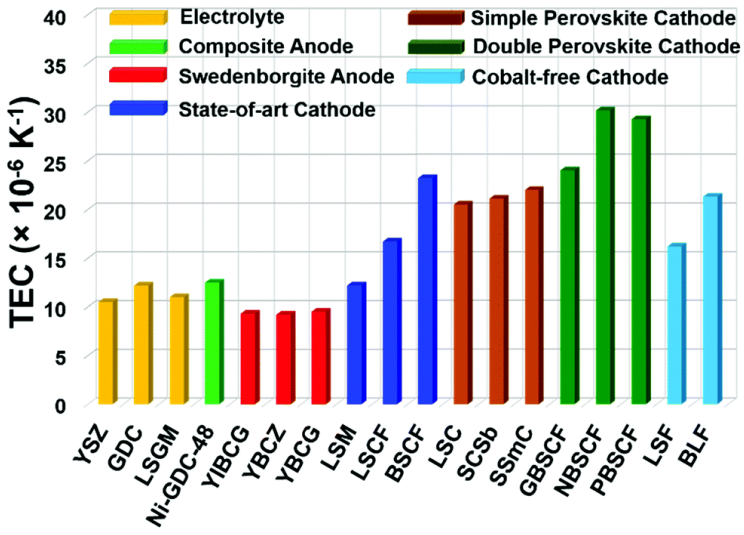

Figure 12: TECs for different SOFC component parts with their various constitutive compositions[186] highlighted as follows: $Zr_{0.84}Y_{0.16}O_{1.92}$ (YSZ)[175], $Ce_{0.8}Gd_{0.2}O_{1.9}$ (GDC) [187],$La_{0.8}Sr_{0.2}Ga_{0.8}Mg_{0.2}O_{3-\delta}$ (LSGM) [188], 48 vol% Ni–GDC (Ni-GDC-48, porous, 75% theoretical density) [189], $Y_{0.9}In_{0.1}BaCo_{3.3}Ga_{0.7}O_{7+\delta}$ (YIBCG) [190], $YBaCo_3ZnO_{7+\delta}$ (YBCZ) [190], $YBaCo_{3.2}Ga_{0.8}O_{7+\delta}$ (YBCG)[190], $La_{0.8}Sr_{0.2}MnO_{3-\delta}$ (LSM)[191], $La_{0.6}Sr_{0.4}Co_{0.2}Fe_{0.8}O_{3-\delta}$ (LSCF)[192], $Ba_{0.5}Sr_{0.5}Co_{0.8}Fe_{0.2}O_{3-\delta}$ (BSCF)[193], $La_{0.6}Sr_{0.4}CoO_{3-\delta}$ (LSC)[194], $SrCo_{0.9}Sb_{0.1}O_{3-\delta}$ (SCSb)[49], $Sr_{0.5}Sm_{0.5}CoO_{3-\delta}$ (SSmC)[195], $GdBa_{0.5}Sr_{0.5}Co_{1.5}Fe_{0.5}O_{5+\delta}$ (GBSCF)[196], $NdBa_{0.5}Sr_{0.5}Co_{1.5}Fe_{0.5}O_{5+\delta}$ (NBSCF)[196], $PrBa_{0.5}Sr_{0.5}Co_{1.5}Fe_{0.5}O_{5+\delta}$ (PBSCF)[196], $La_{0.6}Sr_{0.4}FeO_{3-\delta}$ (LSF) [197], and $Ba_{0.95}La_{0.05}FeO_{3-\delta}$ (BLF) [198].

Figure 134 illustrates a schematic representation of the different TECs for different cathode and electrolyte materials used in P-SOFCs and **Table** provides the details of each electrolyte or cathode compound represented in **Figure 134**.

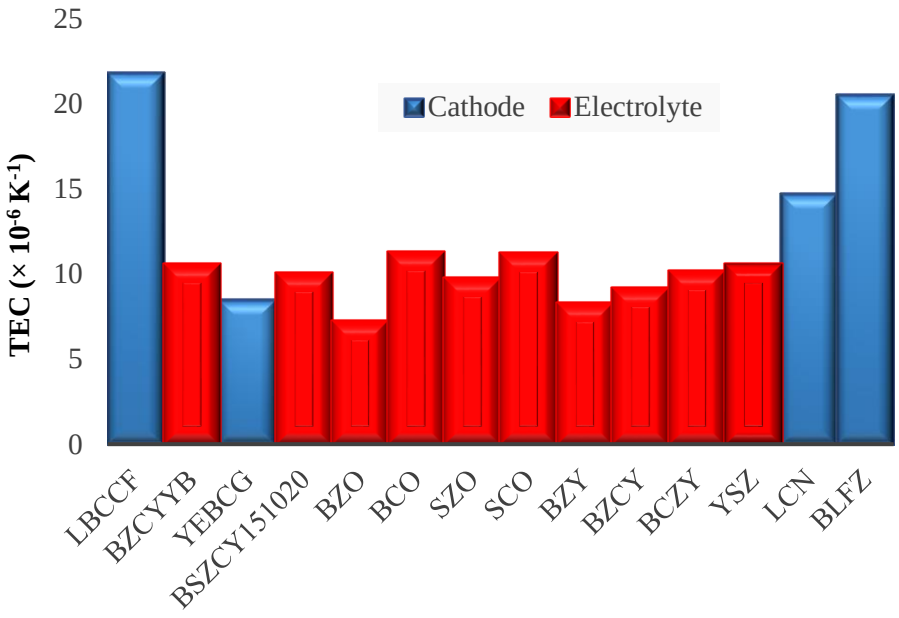

Figure 13: TECs of cathode and electrolyte materials for PCFCs.

Finally, it is also expected that PCFC cathode materials should have high porosity. Although, this porosity is not an intrinsic quality but that achieved by processing. The availability of high porosity will ensure enough transport paths necessary for oxygen and steam molecules diffusion [205].

3.2.5 Self assembled nanocompsite materials design

3.3 Anode materials development for PCFCs

The anode is one of the essential components of a proton-conducting solid oxide fuel cells. However, it has attracted less attention compared to the electrolyte and cathode materials. The anode electrode material for P-SOFC should have both electronic and proton conductivity to increase the number of electrochemically active sites and facilitate an efficient hydrogen oxidation reaction. At the anode, a hydrogen molecule is oxidized to produce two protons and two electrons as illustrated in Equation 4.7.

$$H_2 \rightarrow 2H^+ + 2e^- \qquad (3.7)$$

The design of anode materials for proton-conducting solid oxide fuel cells is like that of oxygen ion conducting solid oxide fuel cells. The P-SOFC anodes are cermets produced by mixing NiO with a proton-conducting electrolyte in which the NiO is subsequently reduced to Ni. This reduction of NiO to Ni consequently leads to the generation of porosity which is necessary for gas diffusion and continuous electronic pathway. The rule of thumb is that a composite anode material is formed by combining an electronic conducting phase (i.e., Ni) with a proton-conducting oxide. Therefore, the proportion of the mixture of the electronic and proton-conducting phases, the microstructure, and particulate size of the anode material is important to be decided carefully because they significantly influence the performance of the cell. The triple-phase boundary increases with an increasing anode surface area which also speeds up the reaction kinetics. This desirable large surface area can be increased by using powders with small average grain sizes. More so, it has been demonstrated that improved symmetric cell performance could be achieved by controlling the anode porosity [206–208].

One of the studies which attempted to gain insights into the reactions at the anode for P-SOFCs with the aim of developing superior anode materials is the research conducted by Pers et al. [206]. They investigated the effect of temperature and atmosphere on the hydrogen oxidation reaction at the Ni-$BaZr_{0\cdot1}Ce_{0\cdot7}Y_{0.1}Yb_{0.1}O_{3-\delta}$ (BZCYYb) interface using impedance spectroscopy at different hydrogen partial pressure in the temperature of 350 – 600 ℃. They asserted that the hydrogen dissociation step is the rate-limiting step for the hydrogen oxidation reaction. Consequently, the polarization resistance of the cermet Ni-BZCYYb was 0.049 Ω cm^2 at *600* ℃ when hydrogen fuel is used.

Also, Essoumhi et al. [209] investigated the microstructure and electrical characteristics of two cermets (ceramic-metal composite) with different Ni content using $BaCe_{0.9}Y_{0.1}O_{2.95}$ ceramic nanopowders. The proportion of Ni in both cermets (i.e., Ni-BCY) is 35 and 45 vol. % which are both equivalents to 50 and 60 wt% NiO. It was discovered that an increase in Ni content improved the porosity and electrical properties of the electrodes.

Chevallier et al. [210] presented a novel wet-chemical route approach for preparing Ni–$BaCe_{0.9}Y_{0.1}O_{3-\delta}$ cermet. This was achieved by dispersing BCY10 nanocrystalline powder in a nickel nitrate solution followed by sintering at a temperature of 1000 ℃. It was found out that the resulting cermet was not tolerant to the CO_2 atmosphere at a temperature of 700 ℃ due to the severe degradation encountered. This renders the use of Ni-BCY anode to be restricted to hydrogen fuel and highly unsuitable for hydrocarbon-based fuels.

Plekhanov et al. [91] investigated suitable and possible anode materials for $LaScO_3$-based proton-conducting electrolytes. Ni-LSS5 cermet was produced via solid-state and co-precipitation methods. They then subjected the LSS5 powder to different production and sintering temperatures in the range of 1400 to 1500 ℃ and observed the microstructural features and phase compositions. It was discovered that the electrical conductivity and chemical expansion of Ni-LSS was majorly influenced by its porosity as opposed to the notion of it being influenced by the various methods of synthesis employed. The porosity and average grain size of the samples were estimated by scanning electron microscopy (SEM) image analysis. It was discovered that as the sintering temperature increases, the porosity decreases as shown in **Figure 14**.

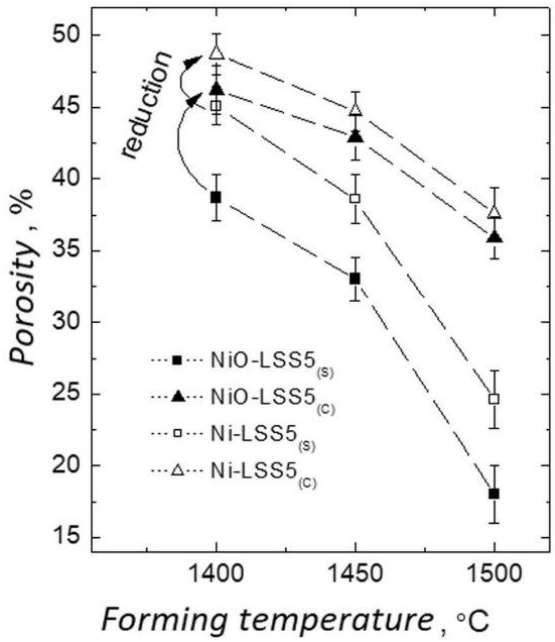

Figure 14: Porosity variation of the various specimens with increasing temperature [91]. Copyright 2021, Springer.

Onishi et al. [211] investigated the performance of Ni-BZY20 cermet used with $BaZr_{0.8}Y_{0.2}O_{3-\delta}$ (BZY20) electrolyte. Ni-BZY20 anode symmetrical cells with a NiO content of 20-70 % were fabricated and tested. They found out that an increase in NiO content made the sintering process more difficult with cells failing at 80 wt% NiO. Hence, it was recommended that the proportion of NiO in the proposed cermet should be less than 70 wt% during cell fabrications.

Ni-based anodes have been vastly employed in SOFCs applications due to their suitability and good performance. However, despite the benefits derived from the use of Ni-based anodes, certain drawbacks have been identified especially when the cell operates at a temperature range of 500 – 800 ℃. [212]. Some of those drawbacks include agglomeration of Ni thereby causing anode performance deterioration with time and coke formation when hydrocarbon fuel is used. Nevertheless, only a few alternatives have been proposed as in several instances where hydrogen-

permeable metal membranes have been used as supporting anodic structure for protonic SOFCs [213,214].

3.3.1 Sintering of PCFC anode materials

Anode-supported cell construction is often employed in most proton-conducting solid oxide fuel cell fabrications. In this form of cell construction, the anode is made the thickest layer of the cell to provide mechanical support for the other cell components. The thick anode layer and the thin electrolyte layer are often co-sintered at a high temperature. The essence of this is to provide the necessary support for the electrolyte and ensure good sinterability by a way of enhancing the quality densification and conductivity of the electrolyte layer. Several studies have highlighted the roles the cermet plays in ensuring quality sintering in P-SOFC electrolytes[36,126,127].

Duan et al. [120] expounded the use of sintering aids such as CuO and NiO to improve the densification of the various electrolytes investigated which were $BaCe_{0.7}Zr_{0.1}Y_{0.1}Yb_{0.1}O_{3-\delta}$ (BCZYYb), $BaZr_{0.8}Y_{0.2}O_{3-\delta}$ (BZY20), and $BaCe_{0.6}Zr_{0.3}Y_{0.1}O_{3-\delta}$ (BCZY63). In order of decreasing stability, we have BZY20 > BCZY63 > BCZYYb. BCZY63 has relatively better sinterability and lower grain boundary resistance while BCZYYb has the highest reported conductivity for P-SOFCs. With a single-cell composition of 40 wt % BCZYYb + 60 wt % NiO | BCZYYb +1.0 wt % NiO | BCZY63 + BCFZY0.1, a peak power density of 0.455 W/cm^2 was achieved at a temperature of 500 ℃ when hydrogen fuel is used.

Furthermore, the sinterability and performance of the anode electrode are also influenced by the morphology of the electrode. For instance, the effect of the quantity of carbon microspheres pore former on the porosity, line shrinkage, electrochemical performance, and thermal expansion of NiO-BCZY71 was investigated. It was discovered that electrode support with 30 wt% pore formers

exhibited the best performance because of its excellent porosity and good triple-phase boundary reactions [215].

4 General synthesis and fabrication of protonic ceramic oxide materials

For years, manufacturing challenges have impeded the development of proton-conducting solid oxide fuel cells until recently when novel methods of synthesizing and fabricating proton-conducting solid oxide fuels emerged. Some of those newly emerged methods for the processing and fabrication of proton-conducting solid oxide fuel cells are solid-state reactive sintering, anode-assisted densification of the electrolyte, extrusion, and interface modification [90].

The synthesis and fabrication of protonic ceramic oxide materials (PCOM) involve several high-temperature and energy-demanding procedures. These procedures are requisite to achieving the desired phases and microstructures as well as other preferable cell component qualities such as porous electrodes, dense electrolytes, and highly stable and durable cells [205]. In a study, it was estimated that materials manufacturing cost accounts for about 30 % of the total proton-conducting solid oxide fuel cell manufacturing cost [125]. Therefore, it is important to devise measures to significantly ameliorate the total manufacturing cost for proton-conducting solid oxide fuel cells by finding alternative and economical fabrication approaches.

Some of the prominently identified measures to significantly reduce PCOM fabrication cost are lowering various material processing temperatures and spotting compositions that do not require expensive precursors (i.e., salts or rare earth oxides). One of the recommended cost-effective methods of synthesizing and fabricating PCOM is solid-state reactive sintering (SSRS)[216]. With this approach, there is a possibility of reducing the arduous and long manufacturing processes from above 10 steps to just 3 or fewer in addition to the consequently reduced sintering temperatures,

time, and energy consumption. What makes the SSRS approach stand out is the fact that it aids the sintering process through the incorporation of a small portion of sintering aids (i.e., NiO, ZnO, CuO, etc.) as expounded in previous sections.

In a study, when 4 wt. % ZnO was added to a well-crystallized BZY powder, a homogeneous distribution of ZnO was produced in the intergranular region. The resulting modified grain boundary composition enhances electrolyte sintering and improves grain growth and boundary mobility caused by an increase in Ba vacancy concentration. Nevertheless, grain boundary conductivity of unmodified BZY is not improved by the introduction of ZnO, rather the grain boundaries are highly tuned. More so, the bulk conductivity of ZnO-modified BZY is relatively lower compared to that of the unmodified BZY. This work gave more insight into the propensity of synthesizing P-SOFCs with lower sintering temperatures and optimized manufacturing processes [217].

Other studies leveraged the foundational concept of SSRS to incorporate phase formation, grain growth, and densification in just a single sintering step which consequently simplified the synthesis and lowered the fabrication cost of P-SOFCs [82,217,218]. Asides from NiO, other sintering aids such as Al_2O_3, LiF, and SnO_2 were investigated to see the one which significantly reduces sintering temperatures. It was found out that NiO is the most effective sintering aid as it reduces the sintering temperature of BZY20 from above 1600 ℃ to 1400 ℃ with a positive densification rating above 95 %[111]. Furthermore, Tong et al. [125]employed a cost-effective SSRS approach to synthesize a high-quality Ni-BZY electrode. A record-breaking conductivity of 0.033 S/cm was achieved at a temperature of 600 ℃ under a wet argon atmosphere. NiO is the most established and widely used sintering aid in the reduction of sintering temperatures for P-SOFCs[28,125–128,219].

Asides from sintering aids, the other factor which influences the effectiveness of SSRS is the nature of the processing. The effect of four different fabrication processes on the conductivity of BZY10 was studied by Ricote et al. [220]. The various fabrication processes include (a) SSRS (b) conventional sintering using powder prepared by solid-state with NiO as the sintering aid (c) conventional sintering using powder prepared by solid-state reaction and then annealing at a high temperature of 2200 ℃ (d) spark plasma sintering (SPS). It was discovered that BZY10 prepared by SSRS as in (a) had the least grain boundary resistance while the resistivity of the other samples using the other fabrication methods in increasing order are: (c), (d) and (b). This confirms that the fabrication process does influence the activation energy for proton conduction across the grain boundaries. This suggests that Ni-decorated grain boundary gotten through SSRS might promote the conduction of proton across grain boundaries. This phenomenon has been confirmed by Clark et al. [221] and Costa et al. [222]. However, Han et al. [223] asserted that the addition of NiO on BZCY based electrolytes affects proton conductivity and dehydration temperature and with time, ionic conductivity will also be affected. Based on this assertion, they concluded that NiO is detrimental to the performance of PCFCs.

Even though tremendous success has been recorded in the adoption and application of the SSRS approach, there are still certain challenges that need to be addressed [224]. One of those challenges is the crossing over of electrons through the electrolyte or leave residual second phases which affect the cell performance. The existence of second phases at grain boundaries may negatively influence the durability of the cell by reducing the mechanical strength of the electrolyte and exposing it to failure. The highlighted challenges however do not obviate the recommendation and application of SSRS in the fabrication of P-SOFCs [120,225]. This is because many highly

efficient and relatively cheaper PCOM have been developed using the SSRS approach thereby confirming the efficacy of this approach in PCOM synthesis and fabrication.

Another important area that is vital to the P-SOFC fabrication process is engineering suitable interfaces between the electrodes and electrolytes. Thermal and chemical incompatibility between the electrodes and electrolytes can result in gradual delamination of P-SOFC parts which will consequently depreciate the cell performance or even lead to failure of the cell. To curb this challenge, some research works have suggested and used interfacial layers to improve the contact between the electrolyte and electrode layers[94,138,154,226–229].

The predominant technique for fabrication of PCOM based cells is through the traditional pressing and co-pressing of perovskite oxide powders. In recent years, researchers have investigated and attempted using tape casting technique for cell fabrication to achieve a larger area, hence higher performance. In 2017, Jin et al.[223] proposed and successfully fabricated an anode supported BZCY based cells by tape casting and suspension spraying. This is an upscale in cell fabrication for PCFCs because it is more established in the traditional O-SOFCs. Hence, more effort is needed in this capacity to further develop ways to achieve meaningful upscale in the fabrication of PCFCs.

5 Prospective for PCFCs

5.1 Identified trends and future guidelines for P-SOFCs

This section presents a summary of recent progress and directions for protonic ceramic fuel cells. Based on the discussions in the previous sections and recent findings, the progress in the advancement of protonic ceramic fuel cells can be highlighted as follows:

(a) There has been an increasing propensity and drive towards more compositionally complex cathode materials which have excellent triple conductivity and are specifically designed for P-SOFCs. More so, it has been observed that most high-performance cathode materials always have an element of Co in their composition. Therefore, it will be prudent to assert that Cobalt containing compounds are promising in achieving a cathode material with an excellent ORR, especially for low and intermediate temperature P-SOFCs.

(b) There has been a dynamic shift from the use of traditional BCY and BZY electrolyte materials to electrolytes with more complex compositions such as BCZYYb and BZCY, with BCZYYb being in the spotlight because of its all-round advantage which involves a balance in the stability, performance, ease of fabrication and performance.

(c) There has been a remarkable improvement in the performance of P-SOFCs using hydrogen fuels from about 0.3 W/cm^2 to 1.302 W/cm^2 at a temperature of 600 ℃ between 2013 and 2019. This represents a hallmark achievement in the advancement of proton-conducting solid oxide fuel cells.

(d) Attention has been driven towards cathode development for PCFCs through the design of self-assembled triple-conducting nanocomposite materials.

(e) There has been an increasing interest in the development of high-performance bifunctional cathode materials which can be used in PCFCs, PCECs, and RePCCs (the RePCC is addressed in section 5.1.1).

One of the important future guidelines is the development of PCFCs with high durability under realistic working conditions. To achieve this, effort need to be intensified to develop P-SOFCs that can function efficiently at temperatures below 400 ℃. A breakthrough in this regard will facilitate the commercialization process for PCFCs.

Hydrogen is an ideal fuel for fuel cells, including H-SOFC. However, hydrogen production and storage efficiently and economically are still challenging. Nevertheless, hydrogen can be generated in the near future through proton conducting electrolysis cells by using excess energy from renewable energy sources such as solar and wind energy. However, conventional hydrocarbon fuels such as natural gas will continue to be a major fuel in the coming decades. Biogas, consisting of methane, hydrogen, carbon monoxide, etc., will increasingly play more important roles in future energy supply. Therefore, it is of practical importance to develop H-SOFC running on conventional hydrocarbon fuels and renewable biogas. Direct hydrocarbon fuel can potentially help in this capacity and several studies have explored and demonstrated this possibility [82,138].

Stability and durability are also important considerations in P-SOFC development. The important roles thermal and chemical stability play in the durability of the cell have been addressed in previous sections. Stability is highly correlated with durability in P-SOFC development.

5.1.1 Reversible protonic ceramic cells

These are energy storage devices that efficiently combine the functionalities of protonic ceramic fuel cells and protonic ceramic electrolysis cells (RePCC). This innovative idea was borne out of

the need to offset the intermittent nature of energy from renewable sources such has wind and solar which have penetrated the energy market in recent years. The excess/waste energy from renewable energy sources during their peak periods can be used to convert electrical energy to chemical energy in the protonic electrolysis cell mode while during periods when the energy demand from the grid exceeds the supply, the stored chemical energy can be converted directly to electrical energy in the protonic ceramic fuel cell mode as illustrated in **Figure 15**. The merits of RePCC are (a) it is relatively economical than chemical batteries on a larger scale, (b) it has a high round trip efficiency, (c) it does not require precious metals as catalysts as in the case of reversible polymer electrolyte membrane electrolysis cells, (d) it directly produces pure and dry hydrogen thereby saving cost and removing complexities associated with drying and external condensers, among others.

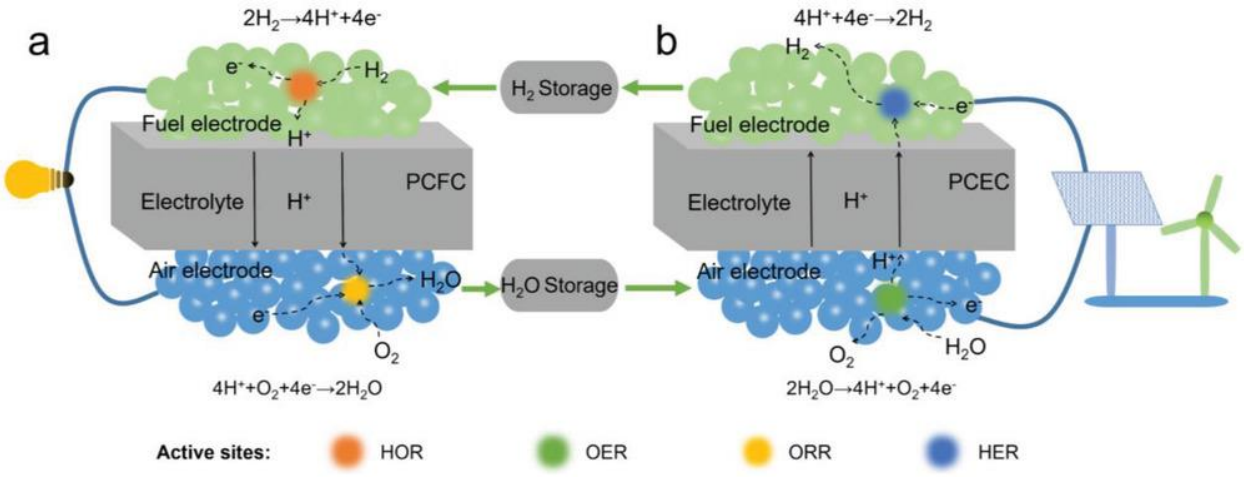

Figure 15: *RePCC operating in (a) protonic ceramic fuel cell mode and (b) protonic ceramic electrolysis mode.* Where HER = hydrogen evolution reaction, ORR = oxygen reduction reaction, OER = oxygen evolution reaction, HOR = hydrogen oxidation reaction [230]. Copyright 2021, John Wiley & Sons.

However, despite the numerous advantages of RePCC, one of the major identified challenges to its commoditization is the paucity in bifunctional electrodes which play a vital role in achieving

highly stable and active electrodes with both excellent oxygen evolution reaction (OER) and oxygen reduction reaction (ORR). High OER in RePCC implies an efficient surface exchange with proton and electron conduction while a high ORR implies a good adsorptive dissociation and diffusion of oxygen, coupled with triple conductivity (i.e., involving protons, electrons, and oxygen ion). All the identified requirements of functional materials cannot be obtained in a single-phase perovskite oxide material. Although some perovskite materials that possess excellent MIEC can be used as air electrodes for RePCC, but they lack proton conductivity and are highly unstable under humid atmospheres [90,231]. Another approach employed for achieving excellent electrode materials for RePCC is the introduction of electronic conductivity into traditional proton conductors such as $BaCeO_3$ and $BaZrO_3$ by doping these materials with transition elements and rare earth metals to achieve materials such as $BaCo_{0.4}Fe_{0.4}Zr_{0.1}Y_{0.1}O_{3-d}$ and $Pr_{0.5}Sr_{0.5}Co_{1.5}Fe_{0.5}O_{5+d}$. Although these materials have excellent performances but there is thermal mismatch between these electrodes and other components of the cell. Hence there need to further consider other material improvement strategies that can cater for these enumerated challenges. Among those strategies considered to achieve this feat is the development of nanocomposite electrodes. Recently, Song et al.[230] presented an interesting and novel perspective based on nanocomposites for advancing bifunctional reversible protonic ceramic cell electrode materials with relatively outstanding performances. Cerium and Nickel Oxide nanoparticles were used to embellish the surface of a nanocomposite electrode comprising Ruddlesden-Popper (RP) and tetragonal perovskite phases. It was discovered that the RP phases enhanced the proton transfer and hydration while the nanoparticles expediated the surface oxygen exchange and transfer of oxide ions from the surface to the major perovskite. This approach promises to create pathway for achieving an optimal reaction activity in electrolysis and fuel cell electrodes.

5.2 PCFC application and scale-up

PCFCs can be employed for stationary applications especially as power supplies for residential devices such as combined heat and power (CHP) cogeneration systems, and other applications such as auxiliary power supplies and power sources for vehicles [232,233]. For these applications to be realized, there is a need for a scale-up. This has been a daunting task particularly due to various stability issues (such as thermal cycling and chemical incompatibility between the cell components) and insufficient knowledge about stack design and system integration [234–237]. There have been attempts to increase the active area of P-SOFCs from 0.5 cm^2 (often used in the labs) to over 50 cm^2 to explore the feasibility of large-scale production [143]. To achieve a scale-up, there must be a significant improvement in material advancement, improved fabrication procedures, and a better understanding of the various key operation mechanisms of the system. In realizing scale-up in PCFCs, some researchers have reported significant contributions that could aid in achieving this goal. For instance, Mu et al. [238] presented a unique digital approach which integrates precise micro extrusion of 3D printing and fast laser processing for achieving several developmental processes in PCFC fabrication such as sintering, drying, cutting and polishing. Tarutin et al. [239] also introduced a one-step sintering process for preparing multilayer PCFCs putting into consideration compatibility of component parts and easier cell preparation methods. Likewise, the use of dynamic mechanical analysis for the characterization of the thermo-mechanical behavior of green tapes have been introduced by Mercadelli et al. [240]. This proposition promises to help achieve optimal lamination viscosity requisite for adhesion between cell component parts regardless of the adopted tape formulation. Scaling up SOFCs and P-SOFCs is very challenging because it requires synergy and expertise contributions from disparate researchers (as observed from some of the scaling up contributing attempts by researchers) from

different disciplines such as Material Science, Mechanical Engineering, Electrical Engineering, Control, and Automation, etc. The aspiration of scale-up in P-SOFC cannot be actualized by a single research group and this makes it even more complicated coupled with the associated costs. Hence, government and philanthropic aids might be required to achieve rapid scale-up in P-SOFC development.

6. Conclusion

The current challenges with the conventional solid oxide fuel cells have driven researchers to consider investigating proton-conducting solid oxide fuel cells as a viable solution to achieving a cleaner, more efficient, and cheaper energy alternative. We have presented a thorough review of the various credible scientific efforts exerted in the development of electrolyte, cathode, and anode materials for PCFCs. Finally, we have buttressed the prospective for PCFCs by highlighting their future guidelines and scale-up potentials.

Acknowledgment

M. Ni thanks the funding support (Project Number: PolyU 152064/18E) from Research Grant Council, University Grants Committee, Hong Kong SAR. B. Chen thanks the National Natural Science Foundation of China Project (No. 52006150) and Natural Science Foundation of Guangdong Province (No. 2020A1515010550). Y. Zhang thanks the fellowship of China postdoctoral science foundation (No. 2021T140471) and the National Natural Science Foundation of China Project (No. 22109101).

References

[1] Günes S, Neugebauer H, Sariciftci NS. Conjugated Polymer-Based Organic Solar Cells. Chem Rev 2007;107:1324–38. https://doi.org/10.1021/cr050149z.

[2] Green MA, Ho-Baillie A, Snaith HJ. The emergence of perovskite solar cells. Nat Photonics 2014;8:506–14. https://doi.org/10.1038/nphoton.2014.134.

[3] Fearnside PM. Dams in the Amazon: Belo Monte and Brazil's Hydroelectric Development of the Xingu River Basin. Environ Manage 2006;38:16. https://doi.org/10.1007/s00267-005-0113-6.

[4] FEARNSIDE PM. Environmental Impacts of Brazil's Tucuruí Dam: Unlearned Lessons for Hydroelectric Development in Amazonia. Environ Manage 2001;27:377–96. https://doi.org/10.1007/s002670010156.

[5] Díaz-González F, Sumper A, Gomis-Bellmunt O, Villafáfila-Robles R. A review of energy storage technologies for wind power applications. Renew Sustain Energy Rev 2012;16:2154–71. https://doi.org/https://doi.org/10.1016/j.rser.2012.01.029.

[6] Joselin Herbert GM, Iniyan S, Sreevalsan E, Rajapandian S. A review of wind energy technologies. Renew Sustain Energy Rev 2007;11:1117–45. https://doi.org/https://doi.org/10.1016/j.rser.2005.08.004.

[7] Barbier E. Geothermal energy technology and current status: an overview. Renew Sustain Energy Rev 2002;6:3–65. https://doi.org/https://doi.org/10.1016/S1364-0321(02)00002-3.

[8] Fridleifsson IB. Geothermal energy for the benefit of the people. Renew Sustain Energy Rev 2001;5:299–312. https://doi.org/https://doi.org/10.1016/S1364-0321(01)00002-8.

[9] Khan MJ, Bhuyan G, Iqbal MT, Quaicoe JE. Hydrokinetic energy conversion systems and assessment of horizontal and vertical axis turbines for river and tidal applications: A technology status review. Appl Energy 2009;86:1823–35. https://doi.org/https://doi.org/10.1016/j.apenergy.2009.02.017.

[10] O Rourke F, Boyle F, Reynolds A. Tidal energy update 2009. Appl Energy 2010;87:398–409. https://doi.org/https://doi.org/10.1016/j.apenergy.2009.08.014.

[11] Notton G, Nivet M-L, Voyant C, Paoli C, Darras C, Motte F, et al. Intermittent and stochastic character of renewable energy sources: Consequences, cost of intermittence and benefit of forecasting. Renew Sustain Energy Rev 2018;87:96–105. https://doi.org/https://doi.org/10.1016/j.rser.2018.02.007.

[12] Merle G, Wessling M, Nijmeijer K. Anion exchange membranes for alkaline fuel cells: A review. J Memb Sci 2011;377:1–35. https://doi.org/https://doi.org/10.1016/j.memsci.2011.04.043.

[13] Varcoe JR, Slade RCT. Prospects for Alkaline Anion-Exchange Membranes in Low Temperature Fuel Cells. Fuel Cells 2005;5:187–200. https://doi.org/https://doi.org/10.1002/fuce.200400045.

[14] Stonehart P. Development of alloy electrocatalysts for phosphoric acid fuel cells (PAFC).

J Appl Electrochem 1992;22:995–1001. https://doi.org/10.1007/BF01029576.

[15] Li Q, Jensen JO, Savinell RF, Bjerrum NJ. High temperature proton exchange membranes based on polybenzimidazoles for fuel cells. Prog Polym Sci 2009;34:449–77. https://doi.org/https://doi.org/10.1016/j.progpolymsci.2008.12.003.

[16] Li H, Tang Y, Wang Z, Shi Z, Wu S, Song D, et al. A review of water flooding issues in the proton exchange membrane fuel cell. J Power Sources 2008;178:103–17. https://doi.org/https://doi.org/10.1016/j.jpowsour.2007.12.068.

[17] Liu H, Song C, Zhang L, Zhang J, Wang H, Wilkinson DP. A review of anode catalysis in the direct methanol fuel cell. J Power Sources 2006;155:95–110. https://doi.org/https://doi.org/10.1016/j.jpowsour.2006.01.030.

[18] Kulkarni A, Giddey S. Materials issues and recent developments in molten carbonate fuel cells. J Solid State Electrochem 2012;16:3123–46. https://doi.org/10.1007/s10008-012-1771-y.

[19] Jacobson AJ. Materials for Solid Oxide Fuel Cells. Chem Mater 2010;22:660–74. https://doi.org/10.1021/cm902640j.

[20] Mahato N, Banerjee A, Gupta A, Omar S, Balani K. Progress in material selection for solid oxide fuel cell technology: A review. Prog Mater Sci 2015;72:141–337. https://doi.org/https://doi.org/10.1016/j.pmatsci.2015.01.001.

[21] Minh NQ. Solid oxide fuel cell technology—features and applications. Solid State Ionics 2004;174:271–7. https://doi.org/https://doi.org/10.1016/j.ssi.2004.07.042.

[22] Laguna-Bercero MA. Recent advances in high temperature electrolysis using solid oxide

fuel cells: A review. J Power Sources 2012;203:4–16. https://doi.org/https://doi.org/10.1016/j.jpowsour.2011.12.019.

[23] Stambouli AB, Traversa E. Solid oxide fuel cells (SOFCs): a review of an environmentally clean and efficient source of energy. Renew Sustain Energy Rev 2002;6:433–55. https://doi.org/https://doi.org/10.1016/S1364-0321(02)00014-X.

[24] Baharuddin NA, Muchtar A, Somalu MR. Short review on cobalt-free cathodes for solid oxide fuel cells. Int J Hydrogen Energy 2017;42:9149–55. https://doi.org/10.1016/j.ijhydene.2016.04.097.

[25] Dong F, Ni M, Chen Y, Chen D, Tadé MO, Shao Z. Structural and oxygen-transport studies of double perovskites PrBa1-xCo2O5+δ (x = 0.00, 0.05, and 0.10) toward their application as superior oxygen reduction electrodes. J Mater Chem A 2014;2:20520–9. https://doi.org/10.1039/c4ta04372c.

[26] Ding P, Li W, Zhao H, Wu C, Zhao L, Dong B, et al. Review on Ruddlesden–Popper perovskites as cathode for solid oxide fuel cells. J Phys Mater 2021;4:022002. https://doi.org/10.1088/2515-7639/abe392.

[27] Ni M, Shao Z. Fuel cells that operate at 300° to 500°C. Science (80-) 2020;369:138 LP – 139. https://doi.org/10.1126/science.abc9136.

[28] Yang G, Su C, Shi H, Zhu Y, Song Y, Zhou W, et al. Toward reducing the operation temperature of solid oxide fuel cells: Our past 15 years of efforts in cathode development. Energy and Fuels 2020;34:15169–94. https://doi.org/10.1021/acs.energyfuels.0c01887.

[29] Leng Y, Chan SH, Liu Q. Development of LSCF–GDC composite cathodes for low-

temperature solid oxide fuel cells with thin film GDC electrolyte. Int J Hydrogen Energy 2008;33:3808–17. https://doi.org/https://doi.org/10.1016/j.ijhydene.2008.04.034.

[30] de Larramendi I, Lamas DG, Cabezas MD, de Larramendi JI, de Reca NE, Rojo T. Development of electrolyte-supported intermediate-temperature single-chamber solid oxide fuel cells using Ln0.7Sr0.3Fe0.8Co0.2O3-δ (Ln = Pr, La, Gd) cathodes. J Power Sources 2009;193:774–8. https://doi.org/10.1016/j.jpowsour.2009.04.069.

[31] Jiang SP. Development of lanthanum strontium manganite perovskite cathode materials of solid oxide fuel cells: A review. J Mater Sci 2008;43:6799–833. https://doi.org/10.1007/s10853-008-2966-6.

[32] Zhou W, Ran R, Shao Z. Progress in understanding and development of Ba0.5Sr0.5Co0.8Fe0.2O3-δ-based cathodes for intermediate-temperature solid-oxide fuel cells: A review. J Power Sources 2009;192:231–46. https://doi.org/10.1016/j.jpowsour.2009.02.069.

[33] He W, Wu X, Yang G, Shi H, Dong F, Ni M. BaCo0.7Fe0.22Y0.08O3-δ as an Active Oxygen Reduction Electrocatalyst for Low-Temperature Solid Oxide Fuel Cells below 600 °c. ACS Energy Lett 2017;2:301–5. https://doi.org/10.1021/acsenergylett.6b00617.

[34] Zhou W, Shao Z, Liang F, Chen Z-G, Zhu Z, Jin W, et al. A new cathode for solid oxide fuel cells capable of in situ electrochemical regeneration. J Mater Chem 2011;21:15343–51. https://doi.org/10.1039/c1jm12660a.

[35] Hashim SS, Liang F, Zhou W, Sunarso J. Cobalt-Free Perovskite Cathodes for Solid Oxide Fuel Cells. ChemElectroChem 2019;6:3549–69. https://doi.org/10.1002/celc.201900391.

[36] Gu H, Ran R, Zhou W, Shao Z. Anode-supported ScSZ-electrolyte SOFC with whole cell materials from combined EDTA-citrate complexing synthesis process. J Power Sources 2007;172:704–12. https://doi.org/10.1016/j.jpowsour.2007.07.056.

[37] Zhang L, Yang W. High-performance low-temperature solid oxide fuel cells using thin proton-conducting electrolyte with novel cathode. Int J Hydrogen Energy 2012;37:8635–40. https://doi.org/10.1016/j.ijhydene.2012.02.140.

[38] Rousseau F, Nickravech M, Awamat S, Morvan D, Amouroux J. Optical emission spectroscopy of a supersonic low-pressure plasma reactor used to synthesis SOFC cathodes thin layers. High Temp Mater Process 2006;10:431–44. https://doi.org/10.1615/HighTempMatProc.v10.i3.70.

[39] Sun W, Yan L, Shi Z, Zhu Z, Liu W. Fabrication and performance of a proton-conducting solid oxide fuel cell based on a thin BaZr0.8Y0.2O3-δ electrolyte membrane. J Power Sources 2010;195:4727–30. https://doi.org/10.1016/j.jpowsour.2010.02.012.

[40] Ju Y-W, Inagaki T, Ida S, Ishihara T. Sm(Sr)CoO3 cone cathode on LaGaO3 thin film electrolyte for IT-SOFC with high power density. J Electrochem Soc 2011;158:B825–30. https://doi.org/10.1149/1.3592427.

[41] Irshad M, Idrees R, Siraj K, Shakir I, Rafique M, Ain QU, et al. Electrochemical evaluation of mixed ionic electronic perovskite cathode LaNi1-xCoxO3-δ for IT-SOFC synthesized by high temperature decomposition. Int J Hydrogen Energy 2020. https://doi.org/10.1016/j.ijhydene.2020.09.180.

[42] Aguadero A, Escudero MJ, Pérez M, Alonso JA, Daza L. Hyperstoichiometric La1.9 Sr0.1 NiO4+δ mixed conductor as novel cathode for intermediate temperature solid oxide

fuel cells. J Fuel Cell Sci Technol 2007;4:294–8. https://doi.org/10.1115/1.2743075.

[43] Huang C, Chen D, Lin Y, Ran R, Shao Z. Evaluation of Ba<inf>0.6</inf>Sr<inf>0.4</inf>Co<inf>0.9</inf>Nb<inf>0.1</inf>O<inf>3-δ</inf> mixed conductor as a cathode for intermediate-temperature oxygen-ionic solid-oxide fuel cells. J Power Sources 2010;195:5176–84. https://doi.org/10.1016/j.jpowsour.2010.02.080.

[44] Irshad M, Idrees R, Siraj K, Shakir I, Rafique M, Ain QU, et al. Electrochemical evaluation of mixed ionic electronic perovskite cathode LaNi1-xCoxO3-δ for IT-SOFC synthesized by high temperature decomposition. Int J Hydrogen Energy 2021;46:10448–56. https://doi.org/10.1016/j.ijhydene.2020.09.180.

[45] Zhen Y, Jiang SP. Characterization and performance of (La,Ba)(Co,Fe)O3 cathode for solid oxide fuel cells with iron-chromium metallic interconnect. J Power Sources 2008;180:695–703. https://doi.org/10.1016/j.jpowsour.2008.02.093.

[46] Rehman SU, Song R-H, Lim T-H, Hong J-E, Lee S-B. Parametric study on electrodeposition of a nanofibrous LaCoO3 SOFC cathode. Ceram Int 2021;47:5570–9. https://doi.org/10.1016/j.ceramint.2020.10.141.

[47] Li M, Wang Y, Wang Y, Chen F, Xia C. Bismuth doped lanthanum ferrite perovskites as novel cathodes for intermediate-temperature solid oxide fuel cells. ACS Appl Mater Interfaces 2014;6:11286–94. https://doi.org/10.1021/am5017045.

[48] Li S, Zhang L, Xia T, Li Q, Sun L, Huo L, et al. Synergistic effect study of EuBa0.98Co2O5+δ-Ce0.8Sm0.2O1.9 composite cathodes for intermediate-temperature solid oxide fuel cells. J Alloys Compd 2019;771:513–21.

https://doi.org/10.1016/j.jallcom.2018.08.300.

[49] Aguadero A, De La Calle C, Alonso JA, Escudero MJ, Fernández-Díaz MT, Daza L. Structural and electrical characterization of the novel SrCo 0.9Sb0.1O3.-δ perovskite: Evaluation as a solid oxide fuel cell cathode material. Chem Mater 2007;19:6437–44. https://doi.org/10.1021/cm071837x.

[50] Zhang Y, Gao X, Sunarso J, Liu B, Zhou W, Ni M, et al. Significantly Improving the Durability of Single-Chamber Solid Oxide Fuel Cells: A Highly Active CO2-Resistant Perovskite Cathode. ACS Appl Energy Mater 2018;1:1337–43. https://doi.org/10.1021/acsaem.8b00051.

[51] Xu C, Sun K, Yang X, Ma M, Ren R, Qiao J, et al. Highly active and CO2-tolerant Sr2Fe1.3Ga0.2Mo0.5O6-δ cathode for intermediate-temperature solid oxide fuel cells. J Power Sources 2020;450. https://doi.org/10.1016/j.jpowsour.2020.227722.

[52] Zhou W, Ran R, Shao Z. Progress in understanding and development of Ba<inf>0.5</inf>Sr<inf>0.5</inf>Co<inf>0.8</inf>Fe<inf>0.2</inf>O<inf>3-δ</inf>-based cathodes for intermediate-temperature solid-oxide fuel cells: A review. J Power Sources 2009;192:231–46. https://doi.org/10.1016/j.jpowsour.2009.02.069.

[53] Shao Z, Haile SM. A high-performance cathode for the next generation of solid-oxide fuel cells. Mater Sustain Energy A Collect Peer-Reviewed Res Rev Artic from Nat Publ Gr 2004;3:255–8. https://doi.org/10.1142/9789814317665_0036.

[54] Pelosato R, Cordaro G, Stucchi D, Cristiani C, Dotelli G. Cobalt based layered perovskites as cathode material for intermediate temperature Solid Oxide Fuel Cells: A brief review. J Power Sources 2015;298:46–67. https://doi.org/10.1016/j.jpowsour.2015.08.034.

[55] Ding H, Xie Y, Xue X. Electrochemical performance of BaZr0.1Ce0.7Y 0.1Yb0.1O3-δ electrolyte based proton-conducting SOFC solid oxide fuel cell with layered perovskite PrBaCo 2O5+δ cathode. J Power Sources 2011;196:2602–7. https://doi.org/10.1016/j.jpowsour.2010.10.069.

[56] Zhao L, Shen J, He B, Chen F, Xia C. Synthesis, characterization and evaluation of PrBaCo2-xFe xO5+δ as cathodes for intermediate-temperature solid oxide fuel cells. Int J Hydrogen Energy 2011;36:3658–65. https://doi.org/10.1016/j.ijhydene.2010.12.064.

[57] Samson Nesaraj A, Dheenadayalan S, Arul Raj I, Pattabiraman R. Wet chemical synthesis and characterization of strontium-doped LaFeO 3 cathodes for an intermediate temperature solid oxide fuel cell application. J Ceram Process Res 2012;13:601–6.

[58] Lou Z, Qiao J, Yan Y, Peng J, Wang Z, Jiang T, et al. Synthesis and characterization of aluminum-doped perovskites as cathode materials for intermediate temperature solid oxide fuel cells. Int J Hydrogen Energy 2012;37:11345–50. https://doi.org/10.1016/j.ijhydene.2012.04.113.

[59] Fabbri E, Bi L, Pergolesi D, Traversa E. High-performance composite cathodes with tailored mixed conductivity for intermediate temperature solid oxide fuel cells using proton conducting electrolytes. Energy Environ Sci 2011;4:4984–93. https://doi.org/10.1039/c1ee02361f.

[60] Le S, Feng Y, Yuan Z, Zhang N, Chi D. Promotion on electrochemical performance of Ba-deficient Ba1 − xBi0.05Co0.8Nb0.15O3 − δ cathode for intermediate temperature solid oxide fuel cells. Int J Energy Res 2019;43:7085–94. https://doi.org/10.1002/er.4731.

[61] Choi S, Yoo S, Shin J-Y, Kim G. High performance SOFC cathode prepared by

infiltration of La n+11NinO3n1 (n 1, 2, and 3) in porous YSZ. J Electrochem Soc 2011;158:B995–9. https://doi.org/10.1149/1.3598170.

[62] Liu T, Li L, Yu J-K. Cathode materials Sr1−xHoxCoO3−Δ (SHC, x ≤ 0.3) for IT-SOFC. Ionics (Kiel) 2016;22:853–8. https://doi.org/10.1007/s11581-015-1614-9.

[63] Meng X, Lü S, Ji Y, Wei T, Zhang Y. Characterization of Pr1-xSrxCo0.8Fe 0.2O3-δ (0.2 ≤ x ≤0.6) cathode materials for intermediate-temperature solid oxide fuel cells. J Power Sources 2008;183:581–5. https://doi.org/10.1016/j.jpowsour.2008.05.052.

[64] Xiao J, Xu Q, Huang D-P, Chen M, Zhao K, Kim B-H. Evaluation of La0.3Ca0.7Fe1−yCryO3−δ (y = 0.1–0.3) cathodes for intermediate temperature solid oxide fuel cells. Mater Res Bull 2017;90:104–10. https://doi.org/10.1016/j.materresbull.2017.02.021.

[65] Shao Q, Ge W, Lu X, Chen Y, Ding Y, Lin B, et al. A promising cathode for proton-conducting intermediate temperature solid oxide fuel cells: Y0.8Ca0.2BaCo4O7+δ. Ceram Int 2015;41:6687–92. https://doi.org/10.1016/j.ceramint.2015.01.090.

[66] Li S, Sun J, Sun X, Zhu B. A high functional cathode material LaNi 0.4Fe 0.6O 3 for low-temperature solid oxide fuel cells. Electrochem Solid-State Lett 2006;9:A86–7. https://doi.org/10.1149/1.2153898.

[67] Rehman AU, Li M, Knibbe R, Khan MS, Peterson VK, Brand HEA, et al. Enhancing Oxygen Reduction Reaction Activity and CO2 Tolerance of Cathode for Low-Temperature Solid Oxide Fuel Cells by in Situ Formation of Carbonates. ACS Appl Mater Interfaces 2019;11:26909–19. https://doi.org/10.1021/acsami.9b07668.

[68] Liu P, Zhu H, Kong J, Wei N, Wang C, Yang X, et al. Preparation and electrochemical properties of Ba<inf>0.8</inf>La<inf>0.2</inf>FeO<inf>3-δ</inf> cathode for intermediate-temperature solid oxide fuel cells. J Sol-Gel Sci Technol 2017;82:233–8. https://doi.org/10.1007/s10971-016-4300-0.

[69] Li Z, Wei B, Lü Z, Zhang Y, Chen K, Miao J, et al. Evaluation of (Ba <inf>0.5</inf>Sr <inf>0.5</inf>) <inf>0.85</inf>Gd <inf>0.15</inf>Co <inf>0.8</inf>Fe <inf>0.2</inf>O <inf>3-δ</inf> cathode for intermediate temperature solid oxide fuel cell. Ceram Int 2012;38:3039–46. https://doi.org/10.1016/j.ceramint.2011.12.001.

[70] Bu Y-F, Zhong Q, Chen D-C, Chen Y, Lai SY, Wei T, et al. A high-performance, cobalt-free cathode for intermediate-temperature solid oxide fuel cells with excellent CO<inf>2</inf> tolerance. J Power Sources 2016;319:178–84. https://doi.org/10.1016/j.jpowsour.2016.04.064.

[71] Wang S, Zheng R, Suzuki A, Hashimoto T. Preparation, thermal expansion and electrical conductivity of La 0.6Sr0.4Co1-xGaxO 3-δ(x=0.0-0.4) as a new cathode material of SOFC. Solid State Ionics 2004;174:157–62. https://doi.org/10.1016/j.ssi.2004.07.029.

[72] Fan L, Su P-C. Layer-structured LiNi0.8Co0.2O2: A new triple (H+/O2-/e-) conducting cathode for low temperature proton conducting solid oxide fuel cells. J Power Sources 2016;306:369–77. https://doi.org/10.1016/j.jpowsour.2015.12.015.

[73] Yao C, Yang J, Zhang H, Chen S, Meng J, Cai K. Characterization of SrFe0.9-xCuxMo0.1O3-δ (x = 0, 0.1 and 0.2) as cathode for intermediate-temperature solid oxide fuel cells. Int J Energy Res 2020. https://doi.org/10.1002/er.6156.

[74] Iwahara H, Esaka T, Uchida H, Maeda N. Proton conduction in sintered oxides and its

application to steam electrolysis for hydrogen production. Solid State Ionics 1981;3–4:359–63. https://doi.org/https://doi.org/10.1016/0167-2738(81)90113-2.

[75] An H, Shin D, Ji H Il. Pr2NiO4+d for cathode in protonic ceramic fuel cells. J Korean Ceram Soc 2018;55:358–63. https://doi.org/10.4191/kcers.2018.55.4.06.

[76] Strandbakke R, Cherepanov VA, Zuev AY, Tsvetkov DS, Argirusis C, Sourkouni G, et al. Gd- and Pr-based double perovskite cobaltites as oxygen electrodes for proton ceramic fuel cells and electrolyser cells. Solid State Ionics 2015;278:120–32. https://doi.org/10.1016/j.ssi.2015.05.014.

[77] Wang Q, Hou J, Fan Y, Xi X-A, Li J, Lu Y, et al. Pr2BaNiMnO7-: δ double-layered Ruddlesden-Popper perovskite oxides as efficient cathode electrocatalysts for low temperature proton conducting solid oxide fuel cells. J Mater Chem A 2020;8:7704–12. https://doi.org/10.1039/c9ta11212j.

[78] Da′as EH, Bi L, Boulfrad S, Traversa E. Nanostructuring the electronic conducting La0.8Sr0.2MnO3−δ cathode for high-performance in proton-conducting solid oxide fuel cells below 600°C. Sci China Mater 2018;61:57–64. https://doi.org/10.1007/s40843-017-9125-1.

[79] Wang P, Xu D, Cheng J, Hong T. Proton uptake kinetics and electromotive force in BaCo0.4Fe0.4Zr0.1Y0.1O3-δ cathode material with e−/O2−/H+ three mobile carriers for protonic ceramic fuel cells. Ionics (Kiel) 2021;27:1185–92. https://doi.org/10.1007/s11581-021-03914-4.

[80] Sun S, Cheng Z. H 2 S Poisoning of Proton Conducting Solid Oxide Fuel Cell and Comparison with Conventional Oxide-Ion Conducting Solid Oxide Fuel Cell . J

Electrochem Soc 2018;165:F836–44. https://doi.org/10.1149/2.0841810jes.

[81] Kreuer KD. Proton-Conducting Oxides. Annu Rev Mater Res 2003;33:333–59. https://doi.org/10.1146/annurev.matsci.33.022802.091825.

[82] Duan C, Tong J, Shang M, Nikodemski S, Sanders M, Ricote S, et al. Readily processed protonic ceramic fuel cells with high performance at low temperatures. Science (80-) 2015;349:1321 LP – 1326. https://doi.org/10.1126/science.aab3987.

[83] Fabbri E, Pergolesi D, Traversa E. Electrode materials: A challenge for the exploitation of protonic solid oxide fuel cells. Sci Technol Adv Mater 2010;11. https://doi.org/10.1088/1468-6996/11/4/044301.

[84] Bello IT, Zhai S, Zhao S, Li Z, Yu N, Ni M. Scientometric review of proton-conducting solid oxide fuel cells. Int J Hydrogen Energy 2021. https://doi.org/10.1016/j.ijhydene.2021.09.061.

[85] Thabet K, Le Gal La Salle A, Quarez E, Joubert O. Protonic-based ceramics for fuel cells and electrolyzers. INC; 2020. https://doi.org/10.1016/b978-0-12-818285-7.00004-6.

[86] Kochetova N, Animitsa I, Medvedev D, Demin A, Tsiakaras P. Recent activity in the development of proton-conducting oxides for high-temperature applications. RSC Adv 2016;6:73222–68. https://doi.org/10.1039/c6ra13347a.

[87] Milewski J, Szczęśniak A, Szabłowski, Bernat R. Key Parameters of Proton-conducting Solid Oxide Fuel Cells from the Perspective of Coherence with Models. Fuel Cells 2020;20:323–31. https://doi.org/10.1002/fuce.201900077.

[88] Rafique M, Nawaz H, Shahid Rafique M, Bilal Tahir M, Nabi G, Khalid NR. Material and

method selection for efficient solid oxide fuel cell anode: Recent advancements and reviews. Int J Energy Res 2019;43:2423–46. https://doi.org/10.1002/er.4210.

[89] Ye Y, Sun X, Zhou M, Chen Y. A mini review on the application of proton-conducting solid oxide cells for CO2 conversion. Energy and Fuels 2020;34:13427–37. https://doi.org/10.1021/acs.energyfuels.0c02899.

[90] Duan C, Huang J, Sullivan N, O'Hayre R. Proton-conducting oxides for energy conversion and storage. Appl Phys Rev 2020;7. https://doi.org/10.1063/1.5135319.

[91] Plekhanov MS, Lesnichyova AS, Stroeva AY, Ananyev M V, Farlenkov AS, Bogdanovich NM, et al. Novel Ni cermets for anode-supported proton ceramic fuel cells. J Solid State Electrochem 2019;23:1389–98. https://doi.org/10.1007/s10008-019-04233-5.

[92] Duan C, Kee RJ, Zhu H, Karakaya C, Chen Y, Ricote S, et al. Highly durable, coking and sulfur tolerant, fuel-flexible protonic ceramic fuel cells. Nature 2018;557:217–22. https://doi.org/10.1038/s41586-018-0082-6.

[93] Sun W, Liu M, Liu W. Chemically stable yttrium and tin co-doped barium zirconate electrolyte for next generation high performance proton-conducting solid oxide fuel cells. Adv Energy Mater 2013;3:1041–50. https://doi.org/10.1002/aenm.201201062.

[94] Fabbri E, Bi L, Tanaka H, Pergolesi D, Traversa E. Chemically stable Pr and y Co-doped barium zirconate electrolytes with high proton conductivity for intermediate-temperature solid oxide fuel cells. Adv Funct Mater 2011;21:158–66. https://doi.org/10.1002/adfm.201001540.

[95] Zhang W, Hu YH. Progress in proton-conducting oxides as electrolytes for low-

temperature solid oxide fuel cells: From materials to devices. Energy Sci Eng 2021;n/a. https://doi.org/https://doi.org/10.1002/ese3.886.

[96] Xu X, Bi L. Proton-conducting electrolyte materials. vol. 96. 2019. https://doi.org/10.1016/B978-0-12-817445-6.00003-X.

[97] Ranran P, Yan W, Lizhai Y, Zongqiang M. Electrochemical properties of intermediate-temperature SOFCs based on proton conducting Sm-doped BaCeO3 electrolyte thin film. Solid State Ionics 2006;177:389–93. https://doi.org/10.1016/j.ssi.2005.11.020.

[98] Katahira K, Kohchi Y, Shimura T, Iwahara H. Protonic conduction in Zr-substituted BaCeO3. Solid State Ionics 2000;138:91–8. https://doi.org/10.1016/S0167-2738(00)00777-3.

[99] Wang CC, Luo D, Jiang SP, Lin B. Highly sulfur poisoning-tolerant BaCeO3-impregnated La0.6Sr0.4Co0.2Fe0.8O3-δ cathodes for solid oxide fuel cells. J Phys D Appl Phys 2018;51. https://doi.org/10.1088/1361-6463/aadf4c.

[100] Yamanaka S, Fujikane M, Hamaguchi T, Muta H, Oyama T, Matsuda T, et al. Thermophysical properties of BaZrO3 and BaCeO3. J Alloys Compd 2003;359:109–13. https://doi.org/https://doi.org/10.1016/S0925-8388(03)00214-7.

[101] Loureiro FJA, Nasani N, Reddy GS, Munirathnam NR, Fagg DP. A review on sintering technology of proton conducting BaCeO3-BaZrO3 perovskite oxide materials for Protonic Ceramic Fuel Cells. J Power Sources 2019;438:226991. https://doi.org/https://doi.org/10.1016/j.jpowsour.2019.226991.

[102] Bi L, Zhang S, Fang S, Tao Z, Peng R, Liu W. A novel anode supported

BaCe0.7Ta0.1Y0.2O3-δ electrolyte membrane for proton-conducting solid oxide fuel cell. Electrochem Commun 2008;10:1598–601. https://doi.org/10.1016/j.elecom.2008.08.024.

[103] Medvedev DA, Lyagaeva JG, Gorbova E V., Demin AK, Tsiakaras P. Advanced materials for SOFC application: Strategies for the development of highly conductive and stable solid oxide proton electrolytes. Prog Mater Sci 2016;75:38–79. https://doi.org/10.1016/j.pmatsci.2015.08.001.

[104] Fabbri E, Pergolesi D, Traversa E. Materials challenges toward proton-conducting oxide fuel cells: A critical review. Chem Soc Rev 2010;39:4355–69. https://doi.org/10.1039/b902343g.

[105] Ma G, Matsumoto H, Iwahara H. Ionic conduction and nonstoichiometry in non-doped BaxCeO3-α. Solid State Ionics 1999;122:237–47. https://doi.org/10.1016/S0167-2738(99)00074-0.

[106] Medvedev D, Murashkina A, Pikalova E, Demin A, Podias A, Tsiakaras P. BaCeO3: Materials development, properties and application. Prog Mater Sci 2014;60:72–129. https://doi.org/10.1016/j.pmatsci.2013.08.001.

[107] Atmospheres W, Bhide S V, Virkar A V. Stability of BaCeO 3 - Based Proton Conductors in Water - Containing Atmospheres Stability of BaCeO 3 -Based Proton Conductors in 1999:3–10.

[108] Bi L, Da'as EH, Shafi SP. Proton-conducting solid oxide fuel cell (SOFC) with Y-doped BaZrO3 electrolyte. Electrochem Commun 2017;80:20–3. https://doi.org/10.1016/j.elecom.2017.05.006.

[109] Hossain S, Abdalla AM, Jamain SNB, Zaini JH, Azad AK. A review on proton conducting electrolytes for clean energy and intermediate temperature-solid oxide fuel cells. Renew Sustain Energy Rev 2017;79:750–64. https://doi.org/10.1016/j.rser.2017.05.147.

[110] Rioja-Monllor L, Bernuy-Lopez C, Fontaine ML, Grande T, Einarsrud MA. Processing of high performance composite cathodes for protonic ceramic fuel cells by exsolution. J Mater Chem A 2019;7:8609–19. https://doi.org/10.1039/c8ta10950h.

[111] Nikodemski S, Tong J, O'Hayre R. Solid-state reactive sintering mechanism for proton conducting ceramics. Solid State Ionics 2013;253:201–10. https://doi.org/https://doi.org/10.1016/j.ssi.2013.09.025.

[112] Han D, Uemura S, Hiraiwa C, Majima M, Uda T. Detrimental Effect of Sintering Additives on Conducting Ceramics: Yttrium-Doped Barium Zirconate. ChemSusChem 2018;11:4102–13. https://doi.org/10.1002/cssc.201801837.

[113] Xia Y, Xu X, Teng Y, Lv H, Jin Z, Wang D, et al. A novel BaFe0.8Zn0.1Bi0.1O3−δ cathode for proton conducting solid oxide fuel cells. Ceram Int 2020;46:25453–9. https://doi.org/10.1016/j.ceramint.2020.07.015.

[114] Wang D, Xia Y, Lv H, Miao L, Bi L, Liu W. PrBaCo2-xTaxO5+δ based composite materials as cathodes for proton-conducting solid oxide fuel cells with high CO2 resistance. Int J Hydrogen Energy 2020;45:31017–26. https://doi.org/10.1016/j.ijhydene.2020.08.094.

[115] LÜ J, WANG L, FAN L, LI Y, DAI L, GUO H. Chemical stability of doped BaCeO3-BaZrO3 solid solutions in different atmospheres. J Rare Earths 2008;26:505–10.

https://doi.org/10.1016/S1002-0721(08)60127-1.

[116] Azad AK, Irvine JTS. Synthesis, chemical stability and proton conductivity of the perovksites Ba(Ce,Zr)1-x Scx O3 - δ. Solid State Ionics 2007;178:635–40. https://doi.org/10.1016/j.ssi.2007.02.004.

[117] Azad AK, Irvine JTS. High density and low temperature sintered proton conductor BaCe 0.5Zr0.35Sc0.1Zn0.05O 3-δ. Solid State Ionics 2008;179:678–82. https://doi.org/10.1016/j.ssi.2008.04.036.

[118] Shi H, Su C, Ran R, Cao J, Shao Z. Electrolyte materials for intermediate-temperature solid oxide fuel cells. Prog Nat Sci Mater Int 2020;30:764–74. https://doi.org/10.1016/j.pnsc.2020.09.003.

[119] Malavasi L, Fisher CAJ, Islam MS. Oxide-ion and proton conducting electrolyte materials for clean energy applications: Structural and mechanistic features. Chem Soc Rev 2010;39:4370–87. https://doi.org/10.1039/b915141a.

[120] Duan C, Tong J, Shang M, Nikodemski S, Sanders M, Ricote S, et al. Readily processed protonic ceramic fuel cells with high performance at low temperatures. Science (80-) 2015;349:1321–6. https://doi.org/10.1126/science.aab3987.

[121] Wang W, Qu J, Julião PSB, Shao Z. Recent Advances in the Development of Anode Materials for Solid Oxide Fuel Cells Utilizing Liquid Oxygenated Hydrocarbon Fuels: A Mini Review. Energy Technol 2019;7:33–44. https://doi.org/10.1002/ente.201700738.

[122] Jarry A, Jackson GS, Crumlin EJ, Eichhorn B, Ricote S. The effect of grain size on the hydration of BaZr0.9Y0.1O3-: δ proton conductor studied by ambient pressure X-ray

photoelectron spectroscopy. Phys Chem Chem Phys 2019;22:136–43. https://doi.org/10.1039/c9cp04335g.

[123] Iguchi F, Yamada T, Sata N, Tsurui T, Yugami H. The influence of grain structures on the electrical conductivity of a BaZr0.95Y0.05O3 proton conductor. Solid State Ionics 2006;177:2381–4. https://doi.org/10.1016/j.ssi.2006.07.008.

[124] Ueno K, Hatada N, Han D, Uda T. Thermodynamic maximum of y doping level in barium zirconate in co-sintering with NiO. J Mater Chem A 2019;7:7232–41. https://doi.org/10.1039/c8ta12245h.

[125] Tong J, Clark D, Bernau L, Sanders M, O'Hayre R. Solid-state reactive sintering mechanism for large-grained yttrium-doped barium zirconate proton conducting ceramics. J Mater Chem 2010;20:6333–41. https://doi.org/10.1039/C0JM00381F.

[126] Tong J, Clark D, Hoban M, O'Hayre R. Cost-effective solid-state reactive sintering method for high conductivity proton conducting yttrium-doped barium zirconium ceramics. Solid State Ionics 2010;181:496–503. https://doi.org/https://doi.org/10.1016/j.ssi.2010.02.008.

[127] Babilo P, Haile SM. Enhanced sintering of yttrium-doped barium zirconate by addition of ZnO. J Am Ceram Soc 2005;88:2362–8. https://doi.org/10.1111/j.1551-2916.2005.00449.x.

[128] Bi L, Fabbri E, Sun Z, Traversa E. Sinteractive anodic powders improve densification and electrochemical properties of BaZr0.8Y0.2O3-δ electrolyte films for anode-supported solid oxide fuel cells. Energy Environ Sci 2011;4:1352–7. https://doi.org/10.1039/c0ee00387e.

[129] Tao S, Irvine JTS. A stable, easily sintered proton-conducting oxide electrolyte for moderate-temperature fuel cells and electrolyzers. Adv Mater 2006;18:1581–4. https://doi.org/10.1002/adma.200502098.

[130] Tao S, Irvine JTS. Conductivity studies of dense yttrium-doped BaZrO3 sintered at 1325 °C. J Solid State Chem 2007;180:3493–503. https://doi.org/10.1016/j.jssc.2007.09.027.

[131] Sun W, Shi Z, Liu M, Bi L, Liu W. An Easily Sintered, Chemically Stable, Barium Zirconate-Based Proton Conductor for High-Performance Proton-Conducting Solid Oxide Fuel Cells. Adv Funct Mater 2014;24:5695–702. https://doi.org/10.1002/adfm.201401478.

[132] Uhlenbruck S, Tietz F, Haanappel V, Sebold D, Buchkremer H-P, Stöver D. Silver incorporation into cathodes for solid oxide fuel cells operating at intermediate temperature. J Solid State Electrochem 2004;8:923–7. https://doi.org/10.1007/s10008-004-0510-4.

[133] Pergolesi D, Fabbri E, D'Epifanio A, Di Bartolomeo E, Tebano A, Sanna S, et al. High proton conduction in grain-boundary-free yttrium-doped barium zirconate films grown by pulsed laser deposition. Nat Mater 2010;9:846–52. https://doi.org/10.1038/nmat2837.

[134] Zuo C, Zha S, Liu M, Hatano M, Uchiyama M. Ba(Zr0.1Ce0.7Y0.2)O3-δ as an electrolyte for low-temperature solid-oxide fuel cells. Adv Mater 2006;18:3318–20. https://doi.org/10.1002/adma.200601366.

[135] Vázquez S, Davyt S, Basbus JF, Soldati AL, Amaya A, Serquis A, et al. Synthesis and characterization of La0.6Sr0.4Fe0.8Cu0.2O3-δ oxide as cathode for Intermediate Temperature Solid Oxide Fuel Cells. J Solid State Chem 2015;228:208–13. https://doi.org/10.1016/j.jssc.2015.04.044.

[136] Basbus JF, Arce MD, Prado FD, Caneiro A, Mogni L V. A high temperature study on thermodynamic, thermal expansion and electrical properties of BaCe0.4Zr0.4Y0.2O3−δ proton conductor. J Power Sources 2016;329:262–7. https://doi.org/10.1016/j.jpowsour.2016.08.083.

[137] Yang L, Wang S, Blinn K, Liu M, Liu Z, Cheng Z, et al. Enhanced Sulfur and Coking. Science (80-) 2009;326:126–9.

[138] Choi S, Kucharczyk CJ, Liang Y, Zhang X, Takeuchi I, Ji H Il, et al. Exceptional power density and stability at intermediate temperatures in protonic ceramic fuel cells. Nat Energy 2018;3:202–10. https://doi.org/10.1038/s41560-017-0085-9.

[139] Taillades G, Dailly J, Taillades-Jacquin M, Mauvy F, Essouhmi A, Marrony M, et al. Intermediate Temperature Anode-Supported Fuel Cell Based on BaCe0.9Y0.1O3 Electrolyte with Novel Pr2NiO4 Cathode. Fuel Cells 2010;10:166–73. https://doi.org/https://doi.org/10.1002/fuce.200900033.

[140] Zunic M, Chevallier L, Deganello F, D'Epifanio A, Licoccia S, Di Bartolomeo E, et al. Electrophoretic deposition of dense BaCe0.9Y0.1O3−x electrolyte thick-films on Ni-based anodes for intermediate temperature solid oxide fuel cells. J Power Sources 2009;190:417–22. https://doi.org/https://doi.org/10.1016/j.jpowsour.2009.01.046.

[141] Bi L, Fabbri E, Sun Z, Traversa E. A novel ionic diffusion strategy to fabricate high-performance anode-supported solid oxide fuel cells (SOFCs) with proton-conducting Y-doped BaZrO3 films. Energy Environ Sci 2011;4:409–12. https://doi.org/10.1039/c0ee00353k.

[142] Pergolesi D, Fabbri E, Traversa E. Chemically stable anode-supported solid oxide fuel

cells based on Y-doped barium zirconate thin films having improved performance. Electrochem Commun 2010;12:977–80. https://doi.org/https://doi.org/10.1016/j.elecom.2010.05.005.

[143] An H, Lee HW, Kim BK, Son JW, Yoon KJ, Kim H, et al. A 5 × 5 cm2 protonic ceramic fuel cell with a power density of 1.3 W cm–2 at 600 °C. Nat Energy 2018;3:870–5. https://doi.org/10.1038/s41560-018-0230-0.

[144] Yuan R, He W, Zhang C, Ni M, Leung MKH. Cobalt free SrFe0.95Nb0.05O3−δ cathode material for proton-conducting solid oxide fuel cells with BaZr0.1Ce0.7Y0.2O3−δ electrolyte. Mater Lett 2017;200:75–8. https://doi.org/https://doi.org/10.1016/j.matlet.2017.04.103.

[145] Chen C, Dong Y, Li L, Wang Z, Liu M, Rainwater BH, et al. High performance of anode supported BaZr0.1Ce0.7Y0.1Yb0.1O3-δ proton-conducting electrolyte micro-tubular cells with asymmetric structure for IT-SOFCs. J Electroanal Chem 2019;844:49–57. https://doi.org/https://doi.org/10.1016/j.jelechem.2019.05.001.

[146] Chen C, Dong Y, Li L, Wang Z, Liu M, Rainwater BH, et al. Electrochemical properties of micro-tubular intermediate temperature solid oxide fuel cell with novel asymmetric structure based on BaZr0.1Ce0.7Y0.1Yb0.1O3−δ proton conducting electrolyte. Int J Hydrogen Energy 2019;44:16887–97. https://doi.org/https://doi.org/10.1016/j.ijhydene.2019.04.264.

[147] Hou J, Miao L, Hui J, Bi L, Liu W, Irvine JTS. A novel: In situ diffusion strategy to fabricate high performance cathodes for low temperature proton-conducting solid oxide fuel cells. J Mater Chem A 2018;6:10411–20. https://doi.org/10.1039/c8ta00859k.

[148] Bello IT, Zhai S, He Q, Xu Q, Ni M. ScienceDirect Scientometric review of advancements in the development of high-performance cathode for low and intermediate temperature solid oxide fuel cells : Three decades in retrospect. Int J Hydrogen Energy 2021. https://doi.org/10.1016/j.ijhydene.2021.05.134.

[149] Sun C, Hui R, Roller J. Cathode materials for solid oxide fuel cells: A review. J Solid State Electrochem 2010;14:1125–44. https://doi.org/10.1007/s10008-009-0932-0.

[150] Darab M, Toprak MS, Syvertsen GE, Muhammed M. Nanoengineered BSCF cathode materials for intermediate-temperature solid-oxide fuel cells. J Electrochem Soc 2009;156:K139–43. https://doi.org/10.1149/1.3142430.

[151] Xi X, Kondo A, Kozawa T, Naito M. LSCF-GDC composite particles for solid oxide fuel cells cathodes prepared by facile mechanical method. Adv Powder Technol 2016;27:646–51. https://doi.org/10.1016/j.apt.2016.02.022.

[152] Zhu C, Liu X, Yi C, Yan D, Su W. Electrochemical performance of PrBaCo2O5+δ layered perovskite as an intermediate-temperature solid oxide fuel cell cathode. J Power Sources 2008;185:193–6. https://doi.org/10.1016/j.jpowsour.2008.06.075.

[153] Jeong C, Lee J-H, Park M, Hong J, Kim H, Son J-W, et al. Design and processing parameters of La2NiO4+δ-based cathode for anode-supported planar solid oxide fuel cells (SOFCs). J Power Sources 2015;297:370–8. https://doi.org/10.1016/j.jpowsour.2015.08.023.

[154] Tarancón A, Burriel M, Santiso J, Skinner SJ, Kilner JA. Advances in layered oxide cathodes for intermediate temperature solid oxide fuel cells. J Mater Chem 2010;20:3799–813. https://doi.org/10.1039/b922430k.

[155] Jiang Z, Xia C, Chen F. Nano-structured composite cathodes for intermediate-temperature solid oxide fuel cells via an infiltration/impregnation technique. Electrochim Acta 2010;55:3595–605. https://doi.org/https://doi.org/10.1016/j.electacta.2010.02.019.

[156] Li L, Jin F, Shen Y, He T. Cobalt-free double perovskite cathode GdBaFeNiO5+δ and electrochemical performance improvement by Ce0.8Sm0.2O1.9 impregnation for intermediate-temperature solid oxide fuel cells. Electrochim Acta 2015;182:682–92. https://doi.org/10.1016/j.electacta.2015.09.146.

[157] Huan D, Shi N, Xie Y, Li X, Wang W, Xue S, et al. Cathode materials for proton-conducting solid oxide fuel cells. INC; 2019. https://doi.org/10.1016/B978-0-12-817445-6.00008-9.

[158] Wu T, Peng R, Xia C. Sm0.5Sr0.5CoO3 - δ-BaCe0.8Sm0.2O3-δ composite cathodes for proton-conducting solid oxide fuel cells. Solid State Ionics 2008;179:1505–8. https://doi.org/10.1016/j.ssi.2007.12.005.

[159] Kim J, Sengodan S, Kwon G, Ding D, Shin J, Liu M, et al. Triple-Conducting Layered Perovskites as Cathode Materials for Proton-Conducting Solid Oxide Fuel Cells. ChemSusChem 2014;7:2811–5. https://doi.org/10.1002/cssc.201402351.

[160] Wang Z, Yang W, Zhu Z, Peng R, Wu X, Xia C, et al. First-principles study of O2 reduction on BaZr1-xCoxO3 cathodes in protonic-solid oxide fuel cells. J Mater Chem A 2014;2:16707–14. https://doi.org/10.1039/c4ta01652a.

[161] Liang M, He F, Zhou C, Chen Y, Ran R, Yang G, et al. Nickel-doped BaCo0.4Fe0.4Zr0.1Y0.1O3-δ as a new high-performance cathode for both oxygen-ion and proton conducting fuel cells. Chem Eng J 2021;420:127717.

https://doi.org/10.1016/j.cej.2020.127717.

[162] Qi H, Zhao Z, Wang X, Tu B, Cheng M. Self-assembled cubic-hexagonal perovskite nanocomposite as intermediate-temperature solid oxide fuel cell cathode. Ceram Int 2020;46:22282–9. https://doi.org/10.1016/j.ceramint.2020.05.307.

[163] Song Y, Chen Y, Wang W, Zhou C, Zhong Y, Yang G, et al. Self-Assembled Triple-Conducting Nanocomposite as a Superior Protonic Ceramic Fuel Cell Cathode. Joule 2019;3:2842–53. https://doi.org/https://doi.org/10.1016/j.joule.2019.07.004.

[164] Mather GC, Muñoz-gil D, Zamudio-garc J, Porras-v M, Marrero-l D, Domingo P. applied sciences Perspectives on Cathodes for Protonic Ceramic Fuel Cells 2021.

[165] Zohourian R, Merkle R, Raimondi G, Maier J. Mixed-Conducting Perovskites as Cathode Materials for Protonic Ceramic Fuel Cells: Understanding the Trends in Proton Uptake. Adv Funct Mater 2018;28:1–10. https://doi.org/10.1002/adfm.201801241.

[166] Papac M, Stevanović V, Zakutayev A, O'Hayre R. Triple ionic–electronic conducting oxides for next-generation electrochemical devices. Nat Mater 2021;20:301–13. https://doi.org/10.1038/s41563-020-00854-8.

[167] Fabbri E, Bi L, Pergolesi D, Traversa E. Towards the next generation of solid oxide fuel cells operating below 600 °c with chemically stable proton-conducting electrolytes. Adv Mater 2012;24:195–208. https://doi.org/10.1002/adma.201103102.

[168] Li W, Guan B, Zhang X, Yan J, Zhou Y, Liu X. New mechanistic insight into the oxygen reduction reaction on Ruddlesden-Popper cathodes for intermediate-temperature solid oxide fuel cells. Phys Chem Chem Phys 2016;18:8502–11.

https://doi.org/10.1039/c6cp00056h.

[169] Boulahya K, Muñoz-Gil D, Gómez-Herrero A, Azcondo MT, Amador U. Eu2SrCo1.5Fe0.5O7 a new promising Ruddlesden-Popper member as a cathode component for intermediate temperature solid oxide fuel cells. J Mater Chem A 2019;7:5601–11. https://doi.org/10.1039/c8ta11254a.

[170] Miao L, Hou J, Gong Z, Jin Z, Liu W. A high-performance cobalt-free Ruddlesden-Popper phase cathode La1·2Sr0·8Ni0·6Fe0·4O4+Δ for low temperature proton-conducting solid oxide fuel cells. Int J Hydrogen Energy 2019;44:7531–7. https://doi.org/10.1016/j.ijhydene.2019.01.255.

[171] Li W, Guan B, Zhang X, Yan J, Zhou Y, Liu X. New mechanistic insight into the oxygen reduction reaction on Ruddlesden-Popper cathodes for intermediate-temperature solid oxide fuel cells. Phys Chem Chem Phys 2016;18:8502–11. https://doi.org/10.1039/c6cp00056h.

[172] Huan D, Zhang L, Li X, Xie Y, Shi N, Xue S, et al. A Durable Ruddlesden-Popper Cathode for Protonic Ceramic Fuel Cells. ChemSusChem 2020;13:4994–5003. https://doi.org/10.1002/cssc.202001168.

[173] Chen Z, Wang J, Huan D, Sun S, Wang G, Fu Z, et al. Tailoring the activity via cobalt doping of a two-layer Ruddlesden-Popper phase cathode for intermediate temperature solid oxide fuel cells. J Power Sources 2017;371:41–7. https://doi.org/10.1016/j.jpowsour.2017.10.011.

[174] Zhang Y, Chen B, Guan D, Xu M, Ran R, Ni M, et al. Thermal-expansion offset for high-performance fuel cell cathodes. Nature 2021;591:246–51. https://doi.org/10.1038/s41586-

021-03264-1.

[175] Zhang Z, Xie D, Ni J, Ni C. Ba2YCu3O6+δ-based cathode material for proton-conducting solid oxide fuel cells. Ceram Int 2021;47:14673–9. https://doi.org/https://doi.org/10.1016/j.ceramint.2021.01.242.

[176] Gu C-Y, Wu X-S, Cao J-F, Hou J, Miao L-N, Xia Y-P, et al. High performance Ca-containing La2-xCaxNiO4+δ(0≤x≤0.75) cathode for proton-conducting solid oxide fuel cells. Int J Hydrogen Energy 2020;45:23422–32. https://doi.org/https://doi.org/10.1016/j.ijhydene.2020.06.106.

[177] Wang Z, Lv P, Yang L, Guan R, Jiang J, Jin F, et al. Ba0.95La0.05Fe0.8Zn0.2O3-δ cobalt-free perovskite as a triple-conducting cathode for proton-conducting solid oxide fuel cells. Ceram Int 2020;46:18216–23. https://doi.org/https://doi.org/10.1016/j.ceramint.2020.04.144.

[178] Wan T-T, Zhu A-K, Li H-B, Wang C-C, Guo Y-M, Shao Z-P, et al. Performance variability of Ba0.5Sr0.5Co0.8Fe0.2O3−δcathode on proton-conducting electrolyte SOFCs with Ag and Au current collectors. Rare Met 2018;37:633–41. https://doi.org/10.1007/s12598-017-0942-5.

[179] Liu Y, Guo Y, Ran R, Shao Z. A novel approach for substantially improving the sinterability of BaZr0.4Ce0.4Y0.2O3−δ electrolyte for fuel cells by impregnating the green membrane with zinc nitrate as a sintering aid. J Memb Sci 2013;437:189–95. https://doi.org/https://doi.org/10.1016/j.memsci.2013.03.002.

[180] Bae K, Noh H-S, Jang DY, Hong J, Kim H, Yoon KJ, et al. High-performance thin-film protonic ceramic fuel cells fabricated on anode supports with a non-proton-conducting

ceramic matrix. J Mater Chem A 2016;4:6395–403. https://doi.org/10.1039/C5TA10670B.

[181] Lin Y, Ran R, Zheng Y, Shao Z, Jin W, Xu N, et al. Evaluation of Ba0.5Sr0.5Co0.8Fe0.2O3−δ as a potential cathode for an anode-supported proton-conducting solid-oxide fuel cell. J Power Sources 2008;180:15–22. https://doi.org/https://doi.org/10.1016/j.jpowsour.2008.02.044.

[182] Lin Y, Ran R, Shao Z. Silver-modified Ba0.5Sr0.5Co0.8Fe0.2O3−δ as cathodes for a proton conducting solid-oxide fuel cell. Int J Hydrogen Energy 2010;35:8281–8. https://doi.org/https://doi.org/10.1016/j.ijhydene.2009.12.017.

[183] Lin Y, Ran R, Zhang C, Cai R, Shao Z. Performance of PrBaCo2O5+δ as a Proton-Conducting Solid-Oxide Fuel Cell Cathode. J Phys Chem A 2010;114:3764–72. https://doi.org/10.1021/jp9042599.

[184] Lin Y, Zhou W, Sunarso J, Ran R, Shao Z. Characterization and evaluation of BaCo0.7Fe0.2Nb0.1O3−δ as a cathode for proton-conducting solid oxide fuel cells. Int J Hydrogen Energy 2012;37:484–97. https://doi.org/https://doi.org/10.1016/j.ijhydene.2011.09.010.

[185] Tsvetkov N, Lu Q, Sun L, Crumlin EJ, Yildiz B. Improved chemical and electrochemical stability of perovskite oxides with less reducible cations at the surface. Nat Mater 2016;15:1010–6. https://doi.org/10.1038/nmat4659.

[186] Lai K-Y, Manthiram A. Effects of trivalent dopants on phase stability and catalytic activity of YBaCo4O7-based cathodes in solid oxide fuel cells. J Mater Chem A 2018;6:16412–20. https://doi.org/10.1039/C8TA01230J.

[187] Hayashi H, Kanoh M, Quan CJ, Inaba H, Wang S, Dokiya M, et al. Thermal expansion of Gd-doped ceria and reduced ceria. Solid State Ionics 2000;132:227–33. https://doi.org/https://doi.org/10.1016/S0167-2738(00)00646-9.

[188] Du Y, Sammes NM, Tompsett GA, Zhang D, Swan J, Bowden M. Extruded Tubular Strontium- and Magnesium-Doped Lanthanum Gallate, Gadolinium-Doped Ceria, and Yttria-Stabilized Zirconia Electrolytes. J Electrochem Soc 2003;150:A74. https://doi.org/10.1149/1.1525268.

[189] Mori M, Yamamoto T, Itoh H, Inaba H, Tagawa H. Thermal Expansion of Nickel-Zirconia Anodes in Solid Oxide Fuel Cells during Fabrication and Operation. J Electrochem Soc 1998;145:1374–81. https://doi.org/10.1149/1.1838468.

[190] Kim J-H, Manthiram A. Low Thermal Expansion RBa(Co,M)4O7 Cathode Materials Based on Tetrahedral-Site Cobalt Ions for Solid Oxide Fuel Cells. Chem Mater 2010;22:822–31. https://doi.org/10.1021/cm9015244.

[191] Mori M. Mechanisms of Thermal Expansion and Shrinkage of La[sub 0.8]Sr[sub 0.2]MnO[sub 3+δ] Perovskites with Different Densities during Thermal Cycling in Air. J Electrochem Soc 2005;152:A732. https://doi.org/10.1149/1.1864312.

[192] Ullmann H, Trofimenko N, Tietz F, Stöver D, Ahmad-Khanlou A. Correlation between thermal expansion and oxide ion transport in mixed conducting perovskite-type oxides for SOFC cathodes. Solid State Ionics 2000;138:79–90. https://doi.org/https://doi.org/10.1016/S0167-2738(00)00770-0.

[193] McIntosh S, Vente JF, Haije WG, Blank DHA, Bouwmeester HJM. Oxygen Stoichiometry and Chemical Expansion of Ba0.5Sr0.5Co0.8Fe0.2O3-δ Measured by in

Situ Neutron Diffraction. Chem Mater 2006;18:2187–93. https://doi.org/10.1021/cm052763x.

[194] Lee KT, Manthiram A. Comparison of Ln0.6 Sr0.4 Co O3-δ (Ln=La, Pr, Nd, Sm, and Gd) as cathode materials for intermediate temperature solid oxide fuel Cells. J Electrochem Soc 2006;153. https://doi.org/10.1149/1.2172572.

[195] Dong F, Chen D, Ran R, Park H, Kwak C, Shao Z. A comparative study of Sm0.5Sr0.5MO3−δ (M = Co and Mn) as oxygen reduction electrodes for solid oxide fuel cells. Int J Hydrogen Energy 2012;37:4377–87. https://doi.org/https://doi.org/10.1016/j.ijhydene.2011.11.150.

[196] Swierczek K, Zheng K, Klimkowicz A. Optimization of Transport Properties of A-Site Ordered LnBa1-xSrxCo2-yFeyO5+ Perovskite-Type Cathode Materials. ECS Trans 2013;57:1993–2001. https://doi.org/10.1149/05701.1993ecst.

[197] Fossdal A, Menon M, Wærnhus I, Wiik K, Einarsrud M-A, Grande T. Crystal Structure and Thermal Expansion of La1−xSrxFeO3−δ Materials. J Am Ceram Soc 2004;87:1952–8. https://doi.org/https://doi.org/10.1111/j.1151-2916.2004.tb06346.x.

[198] Dong F, Chen D, Chen Y, Zhao Q, Shao Z. La-doped BaFeO3-δ perovskite as a cobalt-free oxygen reduction electrode for solid oxide fuel cells with oxygen-ion conducting electrolyte. J Mater Chem 2012;22:15071–9. https://doi.org/10.1039/c2jm31711g.

[199] Xie D, Li K, Yang J, Yan D, Jia L, Chi B, et al. High-performance La0.5(Ba0.75Ca0.25)0.5Co0.8Fe0.2O3-δ cathode for proton-conducting solid oxide fuel cells. Int J Hydrogen Energy 2021;46:10007–14. https://doi.org/https://doi.org/10.1016/j.ijhydene.2020.01.014.

[200] Shin JS, Park H, Park K, Saqib M, Jo M, Kim JH, et al. Activity of layered swedenborgite structured Y0.8Er0.2BaCo3.2Ga0.8O7+: δfor oxygen electrode reactions in at intermediate temperature reversible ceramic cells. J Mater Chem A 2021;9:607–21. https://doi.org/10.1039/d0ta11000k.

[201] Dayaghi AM, Haugsrud R, Stange M, Larring Y, Strandbakke R, Norby T. Increasing the thermal expansion of proton conducting Y-doped BaZrO3 by Sr and Ce substitution. Solid State Ionics 2021;359:115534. https://doi.org/https://doi.org/10.1016/j.ssi.2020.115534.

[202] Tolchard JR, Grande T. Chemical compatibility of candidate oxide cathodes for BaZrO3 electrolytes. Solid State Ionics 2007;178:593–9. https://doi.org/https://doi.org/10.1016/j.ssi.2007.01.018.

[203] Lyagaeva YG, Medvedev DA, Demin AK, Tsiakaras P, Reznitskikh OG. Thermal expansion of materials in the barium cerate-zirconate system. Phys Solid State 2015;57:285–9. https://doi.org/10.1134/S1063783415020250.

[204] Zhu Z, Qian J, Wang Z, Dang J, Liu W. High-performance anode-supported solid oxide fuel cells based on nickel-based cathode and Ba(Zr0.1Ce0.7Y0.2)O3−δ electrolyte. J Alloys Compd 2013;581:832–5. https://doi.org/https://doi.org/10.1016/j.jallcom.2013.07.210.

[205] Yu J, Ran R, Zhong Y, Zhou W, Ni M, Shao Z. Advances in Porous Perovskites: Synthesis and Electrocatalytic Performance in Fuel Cells and Metal–Air Batteries. ENERGY Environ Mater 2020;3:121–45. https://doi.org/https://doi.org/10.1002/eem2.12064.

[206] Pers P, Mao V, Taillades M, Taillades G. Electrochemical behavior and performances of

Ni-BaZr0·1Ce0·7Y0.1Yb0.1O3−δ cermet anodes for protonic ceramic fuel cell. Int J Hydrogen Energy 2018;43:2402–9. https://doi.org/https://doi.org/10.1016/j.ijhydene.2017.12.024.

[207] Taillades G, Batocchi P, Essoumhi A, Taillades M, Jones DJ, Rozière J. Engineering of porosity, microstructure and electrical properties of Ni–BaCe0.9Y0.1O2.95 cermet fuel cell electrodes by gelled starch porogen processing. Microporous Mesoporous Mater 2011;145:26–31. https://doi.org/https://doi.org/10.1016/j.micromeso.2011.04.020.

[208] Zhao F, Virkar A V. Dependence of polarization in anode-supported solid oxide fuel cells on various cell parameters. J Power Sources 2005;141:79–95. https://doi.org/https://doi.org/10.1016/j.jpowsour.2004.08.057.

[209] Essoumhi A, Taillades G, Taillades-Jacquin M, Jones DJ, Rozière J. Synthesis and characterization of Ni-cermet/proton conducting thin film electrolyte symmetrical assemblies. Solid State Ionics 2008;179:2155–9. https://doi.org/https://doi.org/10.1016/j.ssi.2008.07.025.

[210] Chevallier L, Zunic M, Esposito V, Di Bartolomeo E, Traversa E. A wet-chemical route for the preparation of Ni–BaCe0.9Y0.1O3−δ cermet anodes for IT-SOFCs. Solid State Ionics 2009;180:715–20. https://doi.org/https://doi.org/10.1016/j.ssi.2009.03.005.

[211] Onishi T, Han D, Noda Y, Hatada N, Majima M, Uda T. Evaluation of performance and durability of Ni-BZY cermet electrodes with BZY electrolyte. Solid State Ionics 2018;317:127–35. https://doi.org/https://doi.org/10.1016/j.ssi.2018.01.015.

[212] Atkinson A, Barnett S, Gorte RJ, Irvine JTS, McEvoy AJ, Mogensen M, et al. Advanced anodes for high-temperature fuel cells. Nat Mater 2004;3:17–27.

https://doi.org/10.1038/nmat1040.

[213] Yamaguchi S, Shishido T, Yugami H, Yamamoto S, Hara S. Construction of fuel cells based on thin proton conducting oxide electrolyte and hydrogen-permeable metal membrane electrode. Solid State Ionics 2003;162–163:291–6. https://doi.org/https://doi.org/10.1016/S0167-2738(03)00221-2.

[214] Ito N, Iijima M, Kimura K, Iguchi S. New intermediate temperature fuel cell with ultra-thin proton conductor electrolyte. J Power Sources 2005;152:200–3. https://doi.org/https://doi.org/10.1016/j.jpowsour.2005.01.009.

[215] Yang S, Lu Y, Wang Q, Sun C, Ye X, Wen Z. Effects of porous support microstructure enabled by the carbon microsphere pore former on the performance of proton-conducting reversible solid oxide cells. Int J Hydrogen Energy 2018;43:20050–8. https://doi.org/https://doi.org/10.1016/j.ijhydene.2018.09.011.

[216] Braun RJ, Dubois A, Ferguson K, Duan C, Karakaya C, Kee RJ, et al. Development of kW-Scale Protonic Ceramic Fuel Cells and Systems. ECS Trans 2019;91:997–1008. https://doi.org/10.1149/09101.0997ecst.

[217] Babilo P, Haile SM. Enhanced Sintering of Yttrium-Doped Barium Zirconate by Addition of ZnO. J Am Ceram Soc 2005;88:2362–8. https://doi.org/https://doi.org/10.1111/j.1551-2916.2005.00449.x.

[218] Morejudo SH, Zanón R, Escolástico S, Yuste-Tirados I, Malerød-Fjeld H, Vestre PK, et al. Direct conversion of methane to aromatics in a catalytic co-ionic membrane reactor. Science (80-) 2016;353:563 LP – 566. https://doi.org/10.1126/science.aag0274.

[219] Li J, Wang C, Wang X, Bi L. Sintering aids for proton-conducting oxides – A double-edged sword? A mini review. Electrochem Commun 2020;112:106672. https://doi.org/https://doi.org/10.1016/j.elecom.2020.106672.

[220] Ricote S, Bonanos N, Manerbino A, Sullivan NP, Coors WG. Effects of the fabrication process on the grain-boundary resistance in BaZr0.9Y0.1O3-δ. J Mater Chem A 2014;2:16107–15. https://doi.org/10.1039/c4ta02848a.

[221] Clark D, Tong J, Morrissey A, Almansoori A, Reimanis I, O'Hayre R. Anomalous low-temperature proton conductivity enhancement in a novel protonic nanocomposite. Phys Chem Chem Phys 2014;16:5076–80. https://doi.org/10.1039/c4cp00468j.

[222] Costa R, Grünbaum N, Berger M-H, Dessemond L, Thorel A. On the use of NiO as sintering additive for BaCe0,9Y0,1O3−α. Solid State Ionics 2009;180:891–5. https://doi.org/https://doi.org/10.1016/j.ssi.2009.02.018.

[223] Han D, Goto K, Majima M, Uda T. Proton Conductive BaZr0.8-xCexY0.2O3-δ: Influence of NiO Sintering Additive on Crystal Structure, Hydration Behavior, and Conduction Properties. ChemSusChem 2021;14:614–23. https://doi.org/10.1002/cssc.202002369.

[224] Han D, Uemura S, Hiraiwa C, Majima M, Uda T. Detrimental Effect of Sintering Additives on Conducting Ceramics: Yttrium-Doped Barium Zirconate. ChemSusChem 2018;11:4102–13. https://doi.org/https://doi.org/10.1002/cssc.201801837.

[225] Braun RJ, Dubois A, Ferguson K, Duan C, Karakaya C, Kee RJ, et al. Development of kW-Scale Protonic Ceramic Fuel Cells and Systems. ECS Trans 2019;91:997–1008. https://doi.org/10.1149/09101.0997ecst.

[226] Chiara A, Giannici F, Pipitone C, Longo A, Aliotta C, Gambino M, et al. Solid-Solid Interfaces in Protonic Ceramic Devices: A Critical Review. ACS Appl Mater Interfaces 2020;12:55537–53. https://doi.org/10.1021/acsami.0c13092.

[227] Development of Electrode Materials with Matched Thermal Expansion for Solid Oxide Fuel Cells APPROVED BY SUPERVISING COMMITTEE : 2018.

[228] Liu Y, Compson C, Liu M. Nanostructured and functionally graded cathodes for intermediate temperature solid oxide fuel cells. J Power Sources 2004;138:194–8. https://doi.org/10.1016/j.jpowsour.2004.06.035.

[229] Kumar V, Kaur M, Kaur G, Arya SK, Pickrell G. Stacking designs and sealing principles for IT-solid oxide fuel cell. INC; 2019. https://doi.org/10.1016/B978-0-12-817445-6.00011-9.

[230] Song Y, Liu J, Wang Y, Guan D, Seong A, Liang M, et al. Nanocomposites: A New Opportunity for Developing Highly Active and Durable Bifunctional Air Electrodes for Reversible Protonic Ceramic Cells. Adv Energy Mater 2021;2101899:1–9. https://doi.org/10.1002/aenm.202101899.

[231] Yan A, Cheng M, Dong Y, Yang W, Maragou V, Song S, et al. Investigation of a Ba<inf>0.5</inf>Sr<inf>0.5</inf>Co<inf>0.8</inf>Fe<inf>0.2</inf>O<inf>3- δ</inf> based cathode IT-SOFC. I. The effect of CO<inf>2</inf> on the cell performance. Appl Catal B Environ 2006;66:64–71. https://doi.org/10.1016/j.apcatb.2006.02.021.

[232] Dubois A, Ricote S, Braun RJ. Benchmarking the expected stack manufacturing cost of next generation, intermediate-temperature protonic ceramic fuel cells with solid oxide fuel cell technology. J Power Sources 2017;369:65–77.

https://doi.org/https://doi.org/10.1016/j.jpowsour.2017.09.024.

[233] Dubois A, Ricote S, Braun RJ. Comparing the Expected Stack Cost of Next Generation Intermediate Temperature Protonic Ceramic Fuel Cells with Solid Oxide Fuel Cell Technology. ECS Trans 2017;78:1963–72. https://doi.org/10.1149/07801.1963ecst.

[234] Hassan D, Janes S, Clasen R. Proton-conducting ceramics as electrode/electrolyte materials for SOFC's—part I: preparation, mechanical and thermal properties of sintered bodies. J Eur Ceram Soc 2003;23:221–8. https://doi.org/https://doi.org/10.1016/S0955-2219(02)00173-5.

[235] Fehringer G, Janes S, Wildersohn M, Clasen R. Proton—conducting ceramics as electrode/electrolyte—materials for SOFCs: Preparation, mechanical and thermal-mechanical properties of thermal sprayed coatings, material combination and stacks. J Eur Ceram Soc 2004;24:705–15. https://doi.org/https://doi.org/10.1016/S0955-2219(03)00262-0.

[236] Matzke T, Cappadonia M. Proton conductive perovskite solid solutions with enhanced mechanical stability. Solid State Ionics 1996;86–88:659–63. https://doi.org/https://doi.org/10.1016/0167-2738(96)00231-7.

[237] de Vries KJ. Electrical and mechanical properties of proton conducting SrCe0.95Yb0.05O3 − α. Solid State Ionics 1997;100:193–200. https://doi.org/https://doi.org/10.1016/S0167-2738(97)00350-0.

[238] Mu S, Hong Y, Huang H, Ishii A, Lei J, Song Y, et al. A novel laser 3D printing method for the advanced manufacturing of protonic ceramics. Membranes (Basel) 2020;10:1–17. https://doi.org/10.3390/membranes10050098.

[239] Tarutin A, Danilov N, Lyagaeva J, Medvedev D. One-step fabrication of protonic ceramic fuel cells using a convenient tape calendering method. Appl Sci 2020;10. https://doi.org/10.3390/app10072481.

[240] Mercadelli E, Gondolini A, Montaleone D, Pinasco P, Sanson A. Innovative strategy for designing proton conducting ceramic tapes and multilayers for energy applications. J Eur Ceram Soc 2021;41:488–96. https://doi.org/10.1016/j.jeurceramsoc.2020.09.016.

Table 1: The different types of fuel cells with their various distinct features.

Fuel Cell	Electrolyte	Operation Temperature	Power Output	Efficiency	Catalyst	Ref.
Alkaline fuel cell	Potassium hydroxide	60 – 120℃	10 kW – 100 kW	35 – 70 %	Platinum	[12,13]
Phosphoric acid fuel cell	Phosphoric acid	150 – 200℃	< 200 kW	40 – 80 %	Platinum	[14]
Proton exchange membrane fuel cell	Polymer membrane	50 – 80℃	50 – 250 kW	40 – 50 %	Platinum	[15,16]
Direct Methanol Fuel Cell	Polymer membrane	50 – 130℃	100 MW – 1 kW	20 - 55 %	Platinum	[17]

Molten carbonate fuel cell	Molten lithium or potassium carbonate	≈ 650℃	10 kW – 2 MW	60 – 80 %	Nickel	[18]
Solid oxide fuel cell	Ceramics	500 – 1000℃	kW - MW	> 60 %	Nickel and Perovskites	[19–22]

Table 2: Selected electrochemical performances of single cells with P-SOFC electrolyte materials operated under humidified hydrogen and ambient air.

Electrolyte	**Power density (mW cm^{-2})**	**OCV (V)**	**Temp. (℃)**	**Cell configuration (cathode | electrolyte | anode)**	**Ref.**
$BaCe_{0.9}Y_{0.1}O_{3-\delta}$	96	1.145	600	PR_2NiO_4 | BCY10(85μm) | Ni + BCY10	[139]
$BaCe_{0.9}Y_{0.1}O_{3-\delta}$	150	0.98	600	LSCF8282- BCYb10 | BCY10(13.4μm) | Ni + BCY10	[140]
$BaZr_{0.8}Y_{0.2}O_{3-\delta}$	169	0.97	600	PBC- BZYP | BZY20(20μm) | Ni + BZY20	[141]
$BaZr_{0.8}Y_{0.2}O_{3-\delta}$	110	0.99	600	LSCF6428- BCYb10| BZY20(4μm) | Ni + BZY20	[142]
$BaZr_{0.3}Ce_{0.55}Y_{0.15}O_{3-\delta}$	1302	1.056	600	BSCF| BZCY3(5μm) | Ni + BZCY3	[143]
$BaZr_{0.1}Ce_{0.7}Y_{0.1}Yb_{0.1}O_{3-\delta}$	690	1.04	600	NBSCF| BZCYYb1711(14.7μm) | Ni + BZCYYb1711	[137]
$BaZr_{0.4}Ce_{0.4}Y_{0.1}Yb_{0.1}O_{3-\delta}$	1098	1.01	600	PBSCF| BZCYYb441(15μm) | Ni + BZCYYb441	[138]
$BaZr_{0.1}Ce_{0.7}Y_{0.2}O_{3-\delta}$	428	1.01	600	SFNb | BZCY172 (20μm) | Ni + BZCY172	[144]
$BaZr_{0.1}Ce_{0.7}Y_{0.1}Yb_{0.1}O_{3-\delta}$	580	0.95	600	LSM-SDC | BZCYYb1711(12μm) | Ni + BZCYYb1711	[145]
$BaZr_{0.1}Ce_{0.7}Y_{0.1}Yb_{0.1}O_{3-\delta}$	700	0.98	600	LSCF6428-SDC | BZCYYb1711(12μm) | Ni + BZCYYb1711	[146]

For cathode.
LSCF8282- BCYb10 = $La_{0.8}Sr_{0.2}Co_{0.8}Fe_{0.2}O_{3-\delta}$ - $BaCe_{0.9}Yb_{0.1}O_{3-\delta}$; PBC- BZYP = $PrBaCo_2O_{5+\delta}$- $BaZr_{0.7}Y_{0.2}Pr_{0.1}O_{3-\delta}$; LSCF6428 - BCYb10 = $La_{0.6}Sr_{0.4}Co_{0.2}Fe_{0.8}O_{3-\delta}$ - $BaCe_{0.9}Yb_{0.1}O_{3-\delta}$; BSCF = $Ba_{0.5}Sr_{0.5}Co_{0.8}Fe_{0.2}O_{3-\delta}$; NBSCF = $NdBa_{0.5}Sr_{0.5}Co_{1.5}Fe_{0.5}O_{5+\delta}$; PBSCF = $PrBa_{0.5}Sr_{0.5}Co_{1.5}Fe_{0.5}O_{5+\delta}$; SFNb = $SrFe_{0.95}Nb_{0.05}O_{3-\delta}$; LSM-SDC = $La_{0.75}Sr_{0.25}MnO_{3-\delta}$ - $Ce_{0.8}Sm_{0.2}O_{2-\delta}$; LSCF6428-SDC = $La_{0.6}Sr_{0.4}Co_{0.2}Fe_{0.8}O_{3-\delta}$ - $Ce_{0.8}Sm_{0.2}O_{2-\delta}$

Table 3: Basic steps and order of reactions at the cathode for a typical P-SOFC.

Step	**Reaction(s)**	**Description**
1	$O_2(g) \rightarrow O_{2(ad)}$	Molecular oxygen adsorption
2	$O_{2(ad)} \rightarrow 2O_{(ad)}$	Molecular oxygen dissociation of adsorped oxygen from the air
3	$O_{(ad)} + e^- \rightarrow O^-_{(ad)}$; $O_{(ad)} + 2e^- \rightarrow 2O^{2-}_{(ad)}$	Oxygen reduction at the cathode
4	$O_{(ad)} \rightarrow O_{TPB}$ $O^-_{(ad)} \rightarrow O^-_{TPB}$	Surface diffusion at the electrode/electrolyte/oxygen ion boundary
5	$O^-_{bulk} \rightarrow O^-_{TPB}$	Bulk diffusion of oxygen throughout the cathode

6	$2H^{+}_{bulk} \rightarrow 2H^{+}_{TPB}$	Proton migration towards the anode
7	$2H^{+}_{TPB} + O^{2-}_{TPB} \rightarrow OH^{-}_{TPB}$ $OH^{-}_{TPB} + H^{+}_{TPB} \rightarrow H_2O_{TPB}$	Formation of water at the triple-phase boundary
8	$H_2O_{TPB} \rightarrow H_2O_{(g)}$	Evaporation of water

Table 4: Notable cathode materials for proton-conducting solid oxide fuel cells

Cathode	**Conductivity (Scm^{-1})**	**R_p ($\Omega\ cm^2$)**	**PPD ($mW\ cm^{-2}$)**	**Cell configuration**	**Ref.**
$Ba_2YCu_3O_{6+\delta}$	0.48	0.29@650	175	BYC | BZCY | Ni - BZCY	[175]
$La_{1.5}Ca_{0.5}NiO_{4+\delta}$		0.053@ 700℃	923	LCN | BZCY | Ni - BZCY	[176]
$Ba_{0.95}La_{0.05}Fe_{0.8}Zn_{0.2}O_{3-\delta}$		0.08@750℃	329	BLFZ | BZCYYb | Ni - BZCYYb	[177]
$Ba_{0.5}Sr_{0.5}Co_{0.8}Fe_{0.2}O_{3-\delta}$ (BSCF)		0.189@700℃	356@600℃	BSCF|BZCY721|Ni + $BaZr_{0.2}Ce_{0.7}Y_{0.1}O_{3-\delta}$ (BZCY721)	[178]
BSCF			276@600℃	BSCF|BZCY442|Ni + $BaZr_{0.4}Ce_{0.4}Y_{0.2}O_{3-\delta}$ (BZCY442)	[179]

BSCF		508@600℃	BSCF|BZCY305515|Ni + $BaZr_{0.3}Ce_{0.55}Y_{0.15}O_{3-\delta}$ (BZCY305515)	[180]
BSCF	0.5@600℃	380@600℃	BSCF|BCY|Ni + $BaCe_{0.9}Y_{0.1}O_{3-\delta}$ (BCY)	[181]
BSCF–Ag		245@600℃	BSCF–Ag|BZCY811|Ni + $BaZr_{0.1}Ce_{0.8}Y_{0.1}O_{3-\delta}$ (BZCY811)	[182]
$BaCo_{0.4}Fe_{0.4}Zr_{0.1}Y_{0.1}O_{3-\delta}$	0.2@600℃	970@500℃	BCFZY|BZCYYb + NiO (1 wt %)|Ni + $BaZr_{0.1}Ce_{0.7}Y_{0.1}Yb_{0.1}O_{3-\delta}$ (BZCYYb)	[120]
$Ba(Co_{0.4}Fe_{0.4}Zr_{0.1}Y_{0.1})_{0.95}Ni_{0.05}O_{3-\delta}$	0.607@550℃	450@550℃	BCFZYN|BZCYYb4411|Ni + $BaZr_{0.4}Ce_{0.4}Y_{0.1}Yb_{0.1}O_{3-\delta}$	[161]
$PrBaCo_2O_{5+\delta}$		305@600℃	PBC|BZCY721|Ni + BZCY721	[183]
$Ba_{0.9}Co_{0.7}Fe_{0.2}Nb_{0.1}O_{3-\delta}$	0.046@600℃	1062@600℃	BCFNb|BZCY721|Ni + BZCY721	[184]
$PrBa_{0.5}Sr_{0.5}Co_{1.5}Fe_{0.5}O_{5+\delta}$	0.056@600℃	2160@600℃	PBSCF|BZCYYb4411|Ni + $BaZr_{0.4}Ce_{0.4}Y_{0.1}Yb_{0.1}O_{3-\delta}$ (BZCYYb4411)	[138]
$BaCo_{0.7}(Ce_{0.8}Y_{0.2})O_{3-\delta}$	0.1@600℃	1150@600℃	BCCY|BZCYYb|Ni + BZCYYb	[184]

Table 5: TECs of different cathode and electrolyte materials for PCFCs

Material	**Abbrev.**	**TEC ($\times 10^{-6}$) K^{-1}**		**Ref.**
		Cathode	**Electrolyte**	
$La_{0.5}(Ba_{0.75}Ca_{0.25})_{0.5}Co_{0.8}Fe_{0.2}O_{3-\delta}$	LBCCF	21.7		[199]
$BaZr_{0.1}Ce_{0.7}Y_{0.1}Yb_{0.1}O_{3-\delta}$	BZCYYb		10.5	[199]
$Y_{0.8}Er_{0.2}BaCo_{3.2}Ga_{0.8}O_{7+\delta}$	YEBCG	8.41		[200]
$(Ba_{0.85}Sr_{0.15})(Zr_{0.7}Ce_{0.1}Y_{0.2})O_{2.9}$	BSZCY151020		~10	[201]
$BaZrO_3$	BZO		7.13	[100]
$BaCeO_3$	BCO		11.2	[100]
$SrZrO_3$	SZO		9.7	[202]

$SrCeO_3$	SCO		11.1	[202]
$BaZr_{0.80}Y_{0.20}O_{3-d}$	BZY		8.2	[203]
$BaZr_{0.60}Ce_{0.2}Y_{0.2}O_{3-d}$	BZCY		9.1	[203]
$BaZr_{0.1}Ce_{0.7}Y_{0.2}O_{3-d}$	BCZY		10.1	[204]
$Zr_{0.84}Y_{0.16}O_{1.92}$	YSZ		10.5	[175]
$La_{1.5}Ca_{0.5}NiO_{4+\delta}$	LCN	14.6		[176]
$Ba_{0.95}La_{0.05}Fe_{0.8}Zn_{0.2}O_{3-\delta}$	BLFZ	20.4		[177]

Graphical Table of Contents (GTOC)

The review article presents a detailed exposition of the material developmental strategies for the electrolyte, cathode, and anode of PCFCs. The states-of-the-art synthesis and fabrication techniques as well as prospective and scale-up possibilities of PCFCs were thoughtfully and logically presented.

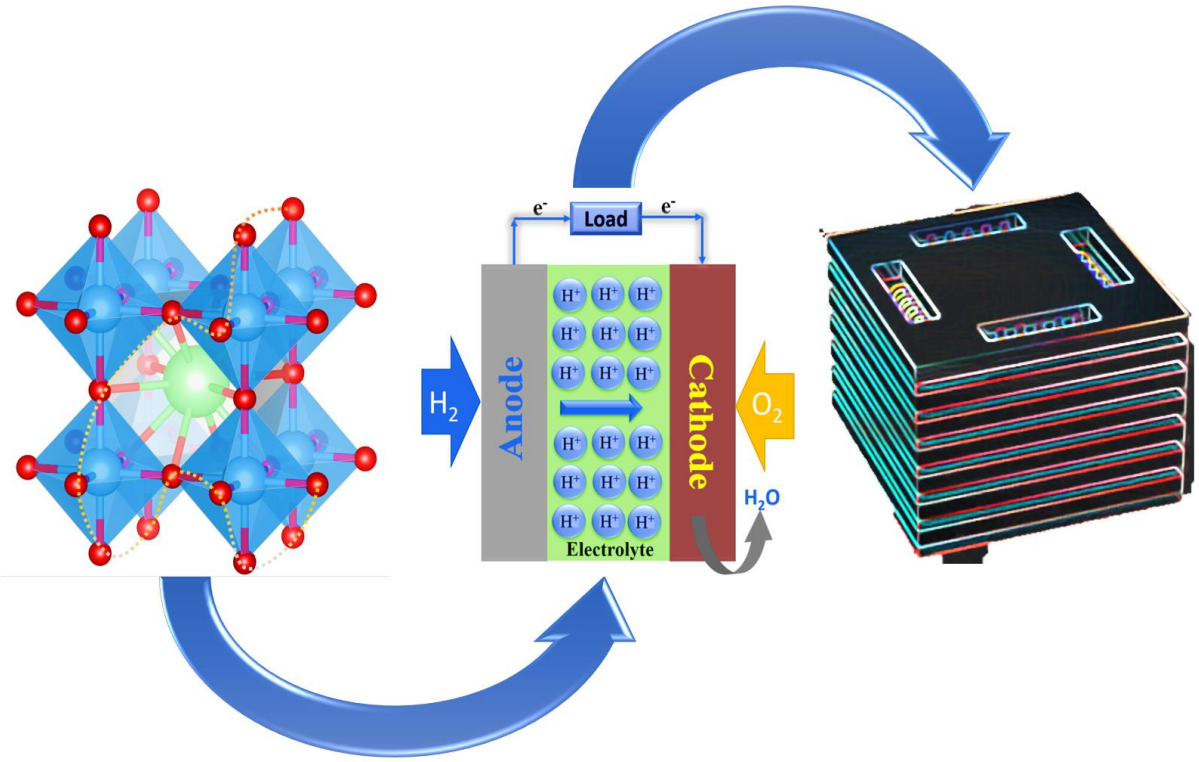
e⁻
Load
e⁻
H₂
Anode
Cathode
O₂
H₂O
Electrolyte